

---

# Spurious Correlation-Aware Embedding Regularization for Worst-Group Robustness

---

**Subeen Park<sup>1</sup>, Joowang Kim<sup>2</sup>, Hakyung Lee<sup>1</sup>, Sunjae Yoo<sup>1</sup>, Kyungwoo Song<sup>1\*</sup>**

<sup>1</sup>Yonsei University, Republic of Korea

<sup>2</sup>LG CNS, Republic of Korea

## Abstract

Deep learning models achieve strong performance across various domains but often rely on spurious correlations, making them vulnerable to distribution shifts. This issue is particularly severe in subpopulation shift scenarios, where models struggle in underrepresented groups. While existing methods have made progress in mitigating this issue, their performance gains are still constrained. They lack a rigorous theoretical framework connecting the embedding space representations with worst-group error. To address this limitation, we propose Spurious Correlation-Aware Embedding Regularization for Worst-Group Robustness (SCER), a novel approach that directly regularizes feature representations to suppress spurious cues. We show theoretically that worst-group error is influenced by how strongly the classifier relies on spurious versus core directions, identified from differences in group-wise mean embeddings across domains and classes. By imposing theoretical constraints at the embedding level, SCER encourages models to focus on core features while reducing sensitivity to spurious patterns. Through systematic evaluation on multiple vision and language, we show that SCER outperforms prior state-of-the-art studies in worst-group accuracy. Our code is available at <https://github.com/MLAI-Yonsei/SCER>.

## 1 Introduction

Deep neural architectures have transformed performance standards in many domains. However, they are still highly vulnerable to spurious correlations in real-world datasets [Yang et al., 2023a, Izmailov et al., 2022, Sagawa et al., 2020]. Spurious correlations refer to patterns in the training data that are statistically associated with target labels without a true causal relationship. Such correlations are often the result of biases in the dataset, causing models to fail when faced with distribution shifts [Ye et al., 2024]. Recent studies have shown that this issue is particularly severe in subpopulation shift scenarios, where the distribution of certain subpopulations in the test data differs from the training distribution [Sagawa et al., Yang et al., 2023b]. Models which are trained with Empirical Risk Minimization (ERM) tend to over-rely on these spurious correlations, as ERM minimizes the average loss without considering subpopulation imbalances [Vapnik, 2013, Izmailov et al., 2022]. As a result, models rely on easily learned but non-robust features, leading to poor worst-group accuracy and unreliable performance on underrepresented subpopulations.

Numerous approaches have been developed to handle this challenge, which can be broadly grouped into several categories [Yang et al., 2023b]. Subpopulation robustness methods [Sagawa et al., Duchi and Namkoong, 2021, Liu et al., 2021, Yao et al., 2022, Deng et al., 2023] focus on improving worst-group performance through various techniques such as reweighting, multi-stage training, or specialized loss functions. Domain invariant methods [Arjovsky et al., 2019, Sun and Saenko, 2016] attempt to learn features that generalize across different domains by aligning feature distributions.

---

\*Corresponding author.

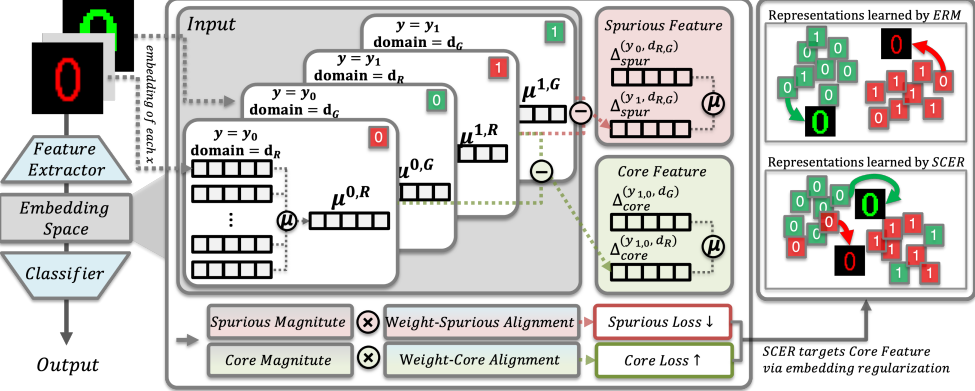


Figure 1: Overview of the Spurious Correlation-Aware Embedding Regularization (SCER) framework. SCER distinguishes spurious and core features via group-wise embedding differences, then regularizes to minimize spurious loss and maximize core loss for domain bias robustness.

Data augmentation approaches [Zhang et al., 2018] create synthetic training examples to improve generalization. Class imbalance methods [Japkowicz, 2000, Cui et al., 2019, Ren et al., 2020] address the uneven distribution of samples across classes. However, these approaches primarily influence model learning indirectly through sample reweighting or feature alignment, without explicitly constraining how spurious features are encoded within the embedding space. Consequently, spurious correlations may persist, limiting robustness under distribution shifts.

To address this limitation, we propose Spurious Correlation-Aware Embedding Regularization for Worst-Group Robustness (SCER), a novel method that directly regularizes feature representations to prevent reliance on spurious features. As illustrated in Figure 1, SCER operates at the embedding level, imposing explicit constraints that guide the model toward learning more robust features. In this study, we provide a new theoretical relationship between worst-group error and the structural properties of representation space under subpopulation shift scenarios, where spurious correlations exist between domain and label. We newly observe two key factors that guarantee the worst-group error from our theoretical analysis. First, for instance, sharing the same label but differing in domain, we regularize their embeddings to capture essential features for classification. Second, for instances sharing the same domain but with different labels, we introduce additional constraints to reduce the impact of domain-specific spurious cues. Through this approach, SCER prevents the model from overfitting to domain-level artifacts, enabling it to learn robust core features more effectively.

By structuring the model’s representation space, SCER improves worst-group accuracy while maintaining strong overall performance. Through extensive experiments on both image and text datasets, we demonstrate that SCER outperforms prior methods in worst-group accuracy. We also provide quantitative and qualitative evidence that embedding-level constraints yield robust feature representations even under spurious domain shifts, confirming the effectiveness of the SCER.

## 2 Related Works

### 2.1 Subpopulation Shift

Machine learning models degrade under subpopulation shift, where test subpopulation distributions differ from training data [Yang et al., 2023b]. ERM’s focus on average training loss makes models susceptible to spurious correlations [Vapnik, 2013, Izmailov et al., 2022]. To address this issue, several approaches have been proposed which can be broadly categorized as sample reweighting and data augmentation strategies. GroupDRO [Sagawa et al.] reduces worst-group error by dynamically upweighting samples from groups with higher loss. LfF [Bahng et al., 2020] employs a two-stage approach that first detects spurious correlations by training a biased model and then debiases a second model by reweighting the loss gradient. GIC [Han and Zou, 2024] improves the accuracy of group inference by leveraging spurious attribute associations. For data augmentation, LISA [Yao et al., 2022] enhances robustness by interpolating between subpopulation samples to encourage invariant representations, while PDE [Deng et al., 2023] gradually expands the training set, allowing models to first learn core features before incorporating more diverse samples. While prior research focuses primarily on sample reweighting or data augmentation, we propose SCER to directly regularize the

embedding space and reduce reliance on spurious features. By explicitly penalizing dependence on spurious cues at the representation level, SCER significantly improves robustness across various distribution shift benchmarks.

## 2.2 Embedding Space

Recent studies in the text and image domains have actively explored methods to refine latent spaces, aiming to improve representation quality and better capture the underlying structure among samples [Patil et al., 2023, Ming et al., 2023]. However, within the domain generalization setting, research has primarily focused on learning invariant features rather than explicitly modifying the embedding space itself. Previous work has attempted to mitigate unintended correlations arising from background, lighting, or dataset-specific biases [Yang et al., 2023b]. Hermann and Lampinen [2020] analyzed how networks differentiate robust and spurious features, while LfF [Bahng et al., 2020] introduced a two-stage training approach to guide model learning. More recently, ElRep [Wen et al., 2025] applies norm penalties to final-layer representations with demonstrated practical effectiveness. However, these methods typically guide model learning indirectly rather than explicitly constraining spurious feature encoding in the embedding space [Patil et al., 2023, Ming et al., 2023]. In contrast to previous approaches, we propose to directly impose an explicit loss function on the embedding space, ensuring that learned representations minimize reliance on spurious correlations and improve generalization under distribution shifts. Our work addresses these theoretical gaps by providing rigorous justification for embedding regularization and establishing clear connections to robust generalization.

## 3 Methodology

### 3.1 Problem Setting

We consider a classification problem where each data point  $x \in \mathcal{X}$  is associated with a label  $y \in \mathcal{Y}$  and a domain  $d \in \mathcal{D}$ , where  $\mathcal{Y} = \{y_1, y_2, \dots, y_m\}$  is the set of  $m$  classes and  $\mathcal{D} = \{d_1, d_2, \dots, d_k\}$  is the set of  $k$  domains. Each pair  $(y, d) \in \mathcal{Y} \times \mathcal{D}$  defines a *subpopulation*, which may exhibit a *spurious correlation* if  $d$  is not causally related to  $y$  but appears disproportionately often with certain  $y$  values. We aim to learn a classifier  $f : \mathcal{X} \rightarrow \mathcal{Y}$ , which consists of a feature extractor  $f_w : \mathcal{X} \rightarrow \mathbb{R}^p$  and a classifier  $f_\beta : \mathbb{R}^p \rightarrow \mathcal{Y}$ , such that  $f(x) = f_\beta(f_w(x))$ . A standard ERM objective aims to minimize

$$\min_f \mathbb{E}_{(x,y) \sim \mathbb{P}} [\ell(f(x), y)],$$

where  $\ell$  is the loss and  $\mathbb{P}$  is the full data distribution. Although ERM effectively reduces *average* error, it can fail on *minority groups*, leading to large misclassification rates in those groups.

**Subpopulation Shift.** We consider a learning setting where performance should remain robust across all subpopulations defined by label-domain pairs  $(y, d)$ . To address imbalances among these groups, we adopt the worst-case optimization framework of Group Distributionally Robust Optimization (GroupDRO), which can be formulated as

$$\min_f \max_{q \in \mathcal{Q}} \sum_{(y,d) \in \mathcal{Y} \times \mathcal{D}} q_{(y,d)} \cdot \mathbb{E}_{(x,y,d) \sim \mathbb{P}_{y,d}} [\ell(f(x), y)]$$

Here,  $\mathbb{P}_{y,d}$  represents the data distribution conditioned on subpopulation  $(y, d)$ ,  $q$  represents how much weight to give each subpopulation during training, and  $\mathcal{Q}$  denotes the set of all possible ways to assign these weights. This minimax formulation ensures robustness across all subpopulations.

To further enhance robustness, we introduce a regularization approach motivated by the geometric decomposition of worst-group error into spurious and core components within the embedding space. Rather than addressing group errors solely through loss optimization, we incorporate structural regularization that encourages the classifier to align with label-consistent **Core Feature** while penalizing dependence on domain-specific **Spurious Feature**. These regularization terms, formulated through directional correlations in the embedding space, are detailed in the following section.

### 3.2 SCER

We propose SCER, which enhances the generalization performance of classifiers by decomposing the worst-group error and applying embedding-level regularization to each component as shown in

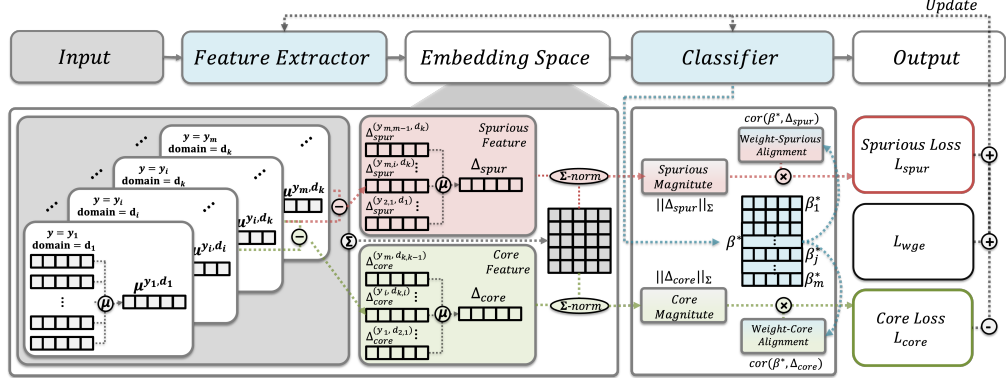


Figure 2: Overview of the SCER training framework. Input data is encoded into embeddings, from which group-wise mean embeddings are computed to derive spurious and core directions. The framework combines worst-group classification loss with embedding regularization that penalizes spurious alignment and promotes core alignment.

Figure 2. Let  $x_{\text{emb}} = f_w(x) \in \mathbb{R}^p$  denote the embedding vectors of input  $x$ , obtained by a feature extractor  $f_w$  with parameters  $w$ , where  $p$  is the embedding dimension. For each subpopulation defined by a label–domain pair  $(y, d)$ , we define its *mean embedding* as

$$\mu^{(y, d)} = \mathbb{E}_{x \sim \mathbb{P}_{y, d}}[f_w(x)] \in \mathbb{R}^p.$$

We compute mean embeddings as representative vectors for each subpopulation, enabling decomposition of worst-group error into two primary components

**Spurious Feature** The embedding mean difference in feature representations across different domains within the same class. Since we assume that label–domain pairs  $(y, d)$  may exhibit spurious correlations, such differences should be minimized to prevent the model from overfitting to domain-specific artifacts. Formally, the spurious difference for a given class  $y$  is defined as

$$\Delta_{\text{spur}}^{(y, d_i, j)} = \left| \mu^{(y, d_i)} - \mu^{(y, d_j)} \right|, \quad \forall y \in \mathcal{Y}, d_i, d_j \in \mathcal{D}, d_i \neq d_j.$$

**Core Feature** The embedding mean difference in feature representations between different classes within the same domain. This quantity captures the true signal that the classifier should leverage for robust prediction. Formally, the core difference for a given domain  $d$  is defined as

$$\Delta_{\text{core}}^{(y_i, j, d)} = \left| \mu^{(y_i, d)} - \mu^{(y_j, d)} \right|, \quad \forall y_i, y_j \in \mathcal{Y}, d \in \mathcal{D}, y_i \neq y_j.$$

The defined  $\Delta_{\text{spur}}^{(y, d_i, j)} \in \mathbb{R}^p$  and  $\Delta_{\text{core}}^{(y_i, j, d)} \in \mathbb{R}^p$  capture key structural variations in the data. To generalize these quantities across multiple classes and domains, we compute global directions using aggregated differences across groups. We define the **Spurious Direction**  $\Delta_{\text{spur}} \in \mathbb{R}^p$  as the average of differences in mean embeddings across domains within the same class, and the **Core Direction**  $\Delta_{\text{core}} \in \mathbb{R}^p$  as the average of differences across classes within the same domain

$$\Delta_{\text{spur}} = \mathbb{E}_{y \in \mathcal{Y}} \left[ \Delta_{\text{spur}}^{(y, d_i, j)} \right], \quad \Delta_{\text{core}} = \mathbb{E}_{d \in \mathcal{D}} \left[ \Delta_{\text{core}}^{(y_i, j, d)} \right],$$

To ensure proper interpretation based on theoretical insights, we normalize these direction vectors using the  $\Sigma$ -norm, defined as  $\|v\|_{\Sigma} = \sqrt{v^{\top} \Sigma v}$  for  $v \in \mathbb{R}^p$ , where  $\Sigma \in \mathbb{R}^{p \times p}$  denotes the empirical covariance matrix of the embedding vectors. This normalization accounts for the geometric structure of the embedding space, producing scalar quantities **Spurious Magnitude**  $\|\Delta_{\text{spur}}\|_{\Sigma}$  and **Core Magnitude**  $\|\Delta_{\text{core}}\|_{\Sigma}$  for use in regularization.

We also derive regularization terms by analyzing how classifier weights align with the Spurious and Core Directions. The key idea is that overreliance on Spurious Directions leads to poor generalization on minority groups, while alignment with Core Directions supports robust performance. Let  $\beta^* = [\beta_1^*, \dots, \beta_j^*, \dots, \beta_m^*] \in \mathbb{R}^{p \times m}$  denote the current weight matrix of the classifier  $f_{\beta}$ , where each column  $\beta_j^* \in \mathbb{R}^p$  corresponds to the weight vector for class  $j$ . During training, we use the current

classifier weights to compute the alignment measures. To quantify the alignment between classifier weights and directional signals, we compute the average class-wise correlation with each direction, using the  $\Sigma$ -norm. We refer to these measures as **Weight-Spurious Alignment** and **Weight-Core Alignment**

$$\text{cor}(\beta^*, \Delta_{\text{spur}}) = \frac{1}{m} \sum_{j=1}^m \frac{\langle \beta_j^*, \Delta_{\text{spur}} \rangle}{\|\beta_j^*\|_\Sigma \cdot \|\Delta_{\text{spur}}\|_\Sigma}, \quad \text{cor}(\beta^*, \Delta_{\text{core}}) = \frac{1}{m} \sum_{j=1}^m \frac{\langle \beta_j^*, \Delta_{\text{core}} \rangle}{\|\beta_j^*\|_\Sigma \cdot \|\Delta_{\text{core}}\|_\Sigma} \quad (1)$$

These correlation terms measure how strongly the classifier's decision boundaries align with spurious or core feature directions, forming the basis of our embedding-level regularization.

Using this definition, we define the Spurious and Core Loss as:

$$\mathcal{L}_{\text{spur}} = \text{cor}(\beta^*, \Delta_{\text{spur}}) \|\Delta_{\text{spur}}\|_\Sigma, \quad \mathcal{L}_{\text{core}} = \text{cor}(\beta^*, \Delta_{\text{core}}) \|\Delta_{\text{core}}\|_\Sigma.$$

The **Spurious Loss**  $\mathcal{L}_{\text{spur}}$  penalizes alignment with spurious directions, scaled by the magnitude of spurious variation in the data. The **Core Loss**  $\mathcal{L}_{\text{core}}$  encourages alignment with core directions, with the negative sign ensuring that stronger core alignment reduces the overall loss. Our loss formulation penalizes alignment with spurious directions and encourages alignment with core directions. By introducing control parameters  $\lambda_{\text{spur}}$  and  $\lambda_{\text{core}}$ , we derive our embedding loss function:

$$\mathcal{L}_{\text{embedding}} = \lambda_{\text{spur}} \mathcal{L}_{\text{spur}} - \lambda_{\text{core}} \mathcal{L}_{\text{core}}. \quad (2)$$

The final SCER objective combines embedding loss with worst-group classification loss  $\mathcal{L}_{\text{wge}}$ :

$$\mathcal{L}_{\text{total}} = \mathcal{L}_{\text{wge}} + \mathcal{L}_{\text{embedding}}. \quad (3)$$

This loss formulation mitigates overfitting to domain-specific biases by reducing intra-class variation across domains while preserving inter-class separability. SCER promotes robust decision boundaries, enabling strong worst-group performance under distribution shifts. For additional implementation details, please refer to Appendix A.1.

### 3.3 Theoretical Analysis of SCER

We now present a theoretical analysis that formally decomposes the worst-group error. Detailed proofs and generalizations are provided in Appendix A.2.

**Theorem 1** (Worst-group Error Decomposition). *Consider a classification problem where each data point  $x \in \mathcal{X}$  is associated with a label  $\mathcal{Y} = \{y_{-1}, y_{+1}\}$  and a domain  $\mathcal{D} = \{d_R, d_G\}$ . Each pair  $(y, d) \in \mathcal{Y} \times \mathcal{D}$  defines a subpopulation. We assume that the data follows a group-conditional Gaussian distribution  $x \mid (y, d) \sim \mathcal{N}(\mu^{(y, d)}, \Sigma)$  where  $\Sigma$  is positive definite. We further assume that  $\Delta_{\text{core}} = \mu^{(y_{+1}, d)} - \mu^{(y_{-1}, d)}$  is constant across  $d$ ,  $\Delta_{\text{spur}} = \mu^{(y, d_R)} - \mu^{(y, d_G)}$  is constant across  $y$ ,  $\Sigma^{(d_R)} = \Sigma^{(d_G)} = \Sigma$ ,  $\mathbb{P}(y = \pm 1) = \mathbb{P}(d \in \{d_R, d_G\}) = \frac{1}{2}$ , and  $\mathbb{P}(y, d) \approx 0$  for some pairs  $(y, d)$  under extreme spurious correlations. For classifier  $f_\beta = \text{sign}(\beta^{*\top} x)$  with  $\beta^* \in \mathbb{R}^p$ , the worst-group error can be decomposed as*

$$E_{\text{wge}} = \Phi\left(\pm \frac{1}{2} \text{cor}(\beta^*, \Delta_{\text{spur}}) \|\Delta_{\text{spur}}\|_\Sigma - \text{cor}(\beta^*, \Delta_{\text{core}}) \|\Delta_{\text{core}}\|_\Sigma\right).$$

**Remark** The sign  $\pm$  appearing in Theorem 1 originates from the fact that the ERM solution Under cross-entropy loss is determined only up to an overall sign. That is, both  $\Sigma^{-1}\tilde{\Delta}$  and  $-\Sigma^{-1}\tilde{\Delta}$  define equivalent solutions, since the classifier depends only on the direction of  $\beta^*$ . Consequently, the  $\pm$  in the expression of the worst-group error does not alter the actual decision boundary or error behavior, but we retain it explicitly to make the sign ambiguity transparent.

The Theorem shows that minimizing  $E_{\text{wge}}$  requires reducing  $\text{cor}(\beta^*, \Delta_{\text{spur}}) \|\Delta_{\text{spur}}\|_\Sigma$  while simultaneously increasing  $\text{cor}(\beta^*, \Delta_{\text{core}}) \|\Delta_{\text{core}}\|_\Sigma$ . The Weight-Spurious Alignment term  $\text{cor}(\beta^*, \Delta_{\text{spur}})$  measures how much the classifier weights align with domain-specific variations within the same class, indicating the dependence on spurious features. The Spurious Magnitude  $\|\Delta_{\text{spur}}\|_\Sigma$  quantifies

Table 1: Performance comparison on multiple datasets, each exhibiting different levels of spurious correlations. For ColorMNIST, we report results under  $\rho = 80\%$ , representing moderate spurious correlation.  $\dagger$  denotes the performance reported from Yang et al. [2023b] except for ColorMNIST.  $\ddagger$  denotes the performance reported from Deng et al. [2023] for Waterbird and CelebA.  $\dagger\dagger$  denotes the performance reported from Wen et al. [2025] for Waterbird and CelebA. For the remaining datasets not cited, detailed experimental settings following Yang et al. [2023b] are described in Appendix B.1.2. SCER achieves the highest worst-group accuracy in Waterbirds, CelebA, MetaShift, and ColorMNIST, demonstrating its robustness in subpopulation shift scenarios.

Algorithm	Waterbirds		CelebA		MetaShift		ColorMNIST	
	Avg Acc	Worst Acc	Avg Acc	Worst Acc	Avg Acc	Worst Acc	Avg Acc	Worst Acc
ERM $\dagger$	84.1 $\pm$ 1.7	69.1 $\pm$ 4.7	95.1 $\pm$ 0.2	62.6 $\pm$ 1.5	91.3 $\pm$ 0.3	82.6 $\pm$ 0.4	38.2 $\pm$ 2.4	30.9 $\pm$ 2.7
Mixup $\dagger$	89.5 $\pm$ 0.4	78.2 $\pm$ 0.4	95.4 $\pm$ 0.1	57.8 $\pm$ 0.8	91.6 $\pm$ 0.3	81.0 $\pm$ 0.8	41.2 $\pm$ 14.0	12.4 $\pm$ 2.0
GroupDRO $\dagger$	88.8 $\pm$ 1.8	78.6 $\pm$ 1.0	91.4 $\pm$ 0.6	89.0 $\pm$ 0.7	91.0 $\pm$ 0.1	85.6 $\pm$ 0.4	73.5 $\pm$ 0.3	73.1 $\pm$ 0.1
IRM $\dagger$	88.4 $\pm$ 0.1	74.5 $\pm$ 1.5	94.7 $\pm$ 0.8	63.0 $\pm$ 2.5	91.8 $\pm$ 0.4	83.0 $\pm$ 0.1	51.6 $\pm$ 11.0	25.0 $\pm$ 6.4
CVaRDRO $\dagger$	89.8 $\pm$ 0.4	75.5 $\pm$ 2.2	95.2 $\pm$ 0.1	64.1 $\pm$ 2.8	92.1 $\pm$ 0.2	84.6 $\pm$ 0.0	42.7 $\pm$ 5.9	30.9 $\pm$ 3.5
JTT $\dagger$	88.8 $\pm$ 0.6	72.0 $\pm$ 0.3	90.4 $\pm$ 2.3	70.0 $\pm$ 10.2	91.2 $\pm$ 0.5	83.6 $\pm$ 0.4	69.1 $\pm$ 1.9	65.2 $\pm$ 4.2
Lff $\dagger$	87.0 $\pm$ 0.3	75.2 $\pm$ 0.7	81.1 $\pm$ 5.6	53.0 $\pm$ 4.3	80.2 $\pm$ 0.3	73.1 $\pm$ 1.6	74.0 $\pm$ 4.1	4.1 $\pm$ 2.3
LISA $\dagger$	92.8 $\pm$ 0.2	88.7 $\pm$ 0.6	92.6 $\pm$ 0.1	86.3 $\pm$ 1.2	89.5 $\pm$ 0.4	84.1 $\pm$ 0.4	73.8 $\pm$ 0.1	73.2 $\pm$ 0.1
MMD $\dagger$	93.0 $\pm$ 0.1	83.9 $\pm$ 1.4	92.5 $\pm$ 0.7	24.4 $\pm$ 2.0	89.4 $\pm$ 0.1	85.9 $\pm$ 0.7	41.7 $\pm$ 0.7	27.5 $\pm$ 7.0
ReSample $\dagger$	89.4 $\pm$ 0.9	77.7 $\pm$ 1.2	92.0 $\pm$ 0.8	87.4 $\pm$ 0.8	91.2 $\pm$ 0.1	85.6 $\pm$ 0.4	73.7 $\pm$ 0.1	72.2 $\pm$ 0.3
ReWeight $\dagger$	91.8 $\pm$ 0.2	86.9 $\pm$ 0.7	91.9 $\pm$ 0.5	89.7 $\pm$ 0.2	91.7 $\pm$ 0.4	85.6 $\pm$ 0.4	74.1 $\pm$ 0.1	73.4 $\pm$ 0.1
SqrReWeight $\dagger$	88.7 $\pm$ 0.3	78.6 $\pm$ 0.1	93.6 $\pm$ 0.1	82.4 $\pm$ 0.5	91.5 $\pm$ 0.2	84.6 $\pm$ 0.7	69.4 $\pm$ 0.7	66.7 $\pm$ 2.0
CBLoss $\dagger$	91.3 $\pm$ 0.7	86.2 $\pm$ 0.3	91.2 $\pm$ 0.7	89.4 $\pm$ 0.7	91.7 $\pm$ 0.4	85.5 $\pm$ 0.4	73.6 $\pm$ 0.2	72.8 $\pm$ 0.2
Focal $\dagger$	89.3 $\pm$ 0.2	71.6 $\pm$ 0.8	94.9 $\pm$ 0.3	59.1 $\pm$ 2.0	91.7 $\pm$ 0.2	81.5 $\pm$ 0.0	40.7 $\pm$ 4.6	31.2 $\pm$ 3.8
LDAM $\dagger$	87.3 $\pm$ 0.5	71.0 $\pm$ 1.8	94.5 $\pm$ 0.2	59.6 $\pm$ 2.4	91.5 $\pm$ 0.1	83.6 $\pm$ 0.4	39.3 $\pm$ 3.1	26.9 $\pm$ 6.1
BSoftmax $\dagger$	88.4 $\pm$ 1.3	74.1 $\pm$ 0.9	91.9 $\pm$ 0.1	83.3 $\pm$ 0.5	91.6 $\pm$ 0.2	83.1 $\pm$ 0.7	40.1 $\pm$ 1.8	33.3 $\pm$ 2.5
DFR $\dagger$	92.3 $\pm$ 0.2	91.0 $\pm$ 0.3	91.9 $\pm$ 0.1	90.4 $\pm$ 0.1	88.4 $\pm$ 0.3	85.4 $\pm$ 0.4	68.4 $\pm$ 0.1	67.3 $\pm$ 0.2
PDE $\ddagger$	92.4 $\pm$ 0.8	90.3 $\pm$ 0.3	92.4 $\pm$ 0.8	91.0 $\pm$ 0.4	87.4 $\pm$ 0.1	78.1 $\pm$ 0.1	76.6 $\pm$ 0.8	72.9 $\pm$ 0.3
ElRep $\dagger\dagger$	92.9 $\pm$ 0.7	88.8 $\pm$ 0.7	92.8 $\pm$ 0.2	91.4 $\pm$ 1.0	85.9 $\pm$ 0.6	72.1 $\pm$ 2.5	50.3 $\pm$ 0.6	46.5 $\pm$ 4.3
SCER	92.1 $\pm$ 0.2	<b>91.2 <math>\pm</math> 0.2</b>	92.7 $\pm$ 0.2	<b>91.4 <math>\pm</math> 0.1</b>	91.6 $\pm$ 0.3	<b>86.7 <math>\pm</math> 0.8</b>	74.1 $\pm$ 0.1	<b>73.6 <math>\pm</math> 0.2</b>

the divergence in the distribution of data between domains within the same label; thus, minimizing this component effectively reduces spurious correlations. In contrast, the Weight-Core Alignment term  $\text{cor}(\beta^*, \Delta_{\text{core}})$  captures how well the classifier weights align with the true labels' discriminatory directions that are consistent across domains. The Core Magnitude  $\|\Delta_{\text{core}}\|_{\Sigma}$  captures the separation between different label distributions across domains, and augmenting this term enhances the model's ability to detect core predictive patterns.

## 4 Experiment

### 4.1 Experiment Setting

**Datasets** We evaluate on both real-world and synthetic datasets. For vision tasks, we use Waterbirds [Sagawa et al.], CelebA [Liu et al., 2015], MetaShift [Liang and Zou, 2022], and ColorMNIST [Arjovsky et al., 2019]. For language tasks, we use CivilComments [Borkan et al., 2019] and MultiNLI [Williams et al., 2017]. These datasets are widely adopted benchmarks for evaluating robustness to spurious correlations. Detailed descriptions and statistics are in Appendix B.1.1.

**Models** Following prior work [Gulrajani and Lopez-Paz, 2020, Izmailov et al., 2022], we use pretrained ResNet-50 [He et al., 2016] for image datasets and pretrained BERT [Idrissi et al., 2022] for text datasets. We use SGD with momentum [Polyak, 1964] for images and AdamW [Loshchilov and Hutter, 2019] for text, following standard protocols [Yang et al., 2023b]. Training steps are 5,000 for Waterbirds, MetaShift, and ColorMNIST, and 30,000 for CelebA, CivilComments, and MultiNLI.

**Baselines** We evaluate our method against various bias mitigation and imbalanced learning algorithms. Our comparison includes ERM; subpopulation robustness methods such as GroupDRO [Sagawa et al.], CVaRDRO [Duchi and Namkoong, 2021], Lff [Nam et al., 2020], JTT [Liu et al., 2021], LISA [Yao et al., 2022], DFR [Kirichenko et al.], PDE [Deng et al., 2023], and ElRep [Wen et al., 2025]; data augmentation approaches including Mixup [Zhang et al., 2018]; domain adaptation methods such as IRM [Arjovsky et al., 2019] and MMD [Li et al., 2018]; and class imbalance techniques including ReSample [Japkowicz, 2000], ReWeight [Japkowicz, 2000], SqrReWeight, Focal Loss [Lin et al., 2017], CB Loss [Cui et al., 2019], LDAM [Cao et al., 2019], and Balanced

Table 2: Performance comparison on ColorMNIST under increasing spurious correlation levels. SCER achieves the highest worst-group accuracy across different spurious correlation levels, demonstrating robustness to spurious feature reliance in ColorMNIST.

Algorithm	ColorMNIST						
	$\rho = 80\%$		$\rho = 90\%$		$\rho = 95\%$		Worst Acc
	Avg Acc	Worst Acc	Avg Acc	Worst Acc	Avg Acc		
ERM	38.2 $\pm$ 2.4	30.9 $\pm$ 2.7	31.9 $\pm$ 7.4	7.8 $\pm$ 3.4	41.1 $\pm$ 13.0	10.1 $\pm$ 4.5	
GroupDRO	73.5 $\pm$ 0.3	73.1 $\pm$ 0.1	73.5 $\pm$ 0.0	72.7 $\pm$ 0.3	72.3 $\pm$ 0.1	70.7 $\pm$ 0.2	
LISA	73.8 $\pm$ 0.1	73.2 $\pm$ 0.1	73.3 $\pm$ 0.1	72.9 $\pm$ 0.2	72.6 $\pm$ 0.4	71.4 $\pm$ 0.6	
ReSample	73.7 $\pm$ 0.1	72.2 $\pm$ 0.3	72.6 $\pm$ 0.5	70.8 $\pm$ 1.6	71.8 $\pm$ 0.1	70.7 $\pm$ 0.5	
ReWeight	74.1 $\pm$ 0.1	73.4 $\pm$ 0.1	73.6 $\pm$ 0.0	72.8 $\pm$ 0.2	72.4 $\pm$ 0.5	70.7 $\pm$ 1.1	
CBLoss	73.6 $\pm$ 0.2	72.8 $\pm$ 0.2	72.7 $\pm$ 0.2	71.7 $\pm$ 0.1	71.8 $\pm$ 0.3	70.8 $\pm$ 0.3	
PDE	76.6 $\pm$ 0.8	72.9 $\pm$ 0.3	72.6 $\pm$ 0.2	70.2 $\pm$ 0.7	73.4 $\pm$ 0.4	70.0 $\pm$ 0.3	
SCER	74.1 $\pm$ 0.1	<b>73.6 <math>\pm</math> 0.2</b>	73.6 $\pm$ 0.1	<b>73.0 <math>\pm</math> 0.1</b>	73.5 $\pm$ 0.3	<b>72.8 <math>\pm</math> 0.3</b>	

Softmax [Ren et al., 2020]. For ColorMNIST, we evaluate only methods that achieve worst-group accuracy above 70%. Detailed experimental settings are provided in Appendix B.1.2.

**Evaluation Metrics** Following prior work, we use Worst-group Accuracy (Worst Acc) as the primary metric to assess performance on the most vulnerable minority group, and Average Accuracy (Avg Acc) for overall performance. Our objective is to minimize the gap between these metrics.

## 5 Results

### 5.1 Quantitative Analysis

**Image Dataset** Table 1 shows that SCER outperforms baseline methods across four benchmarks: Waterbirds, CelebA, MetaShift, and ColorMNIST, each presenting different spurious correlation challenges. SCER achieves the highest worst-group accuracy in four datasets, with 91.2% on Waterbirds, 91.4% on CelebA, 86.7% on MetaShift, and 73.6% on ColorMNIST at  $\rho = 80\%$ . These results demonstrate that embedding-level disentanglement of spurious and core features effectively mitigates bias.

**Image Dataset with Stronger Spurious Correlations** Table 2 reports performance on ColorMNIST under varying levels of spurious correlation  $\rho$ . As  $\rho$  increases, the dataset becomes increasingly biased, making classification more challenging and highlighting the detrimental impact of spurious correlations on standard models. SCER consistently achieves the highest worst-group accuracy across all values of  $\rho$ , attaining 73.6% at  $\rho = 80\%$ , 73.0% at  $\rho = 90\%$ , and 72.8% at  $\rho = 95\%$ , outperforming all baselines.

Table 3: Performance on ColorMNIST with one group absent. SCER achieves the highest worst-group accuracy.

ColorMNIST (One Subpopulation Omitted)		
Algorithm	Avg Acc	Worst Acc
ERM	52.9 $\pm$ 8.4	9.7 $\pm$ 5.4
GroupDRO	53.6 $\pm$ 2.5	44.1 $\pm$ 6.2
LISA	49.5 $\pm$ 2.4	13.5 $\pm$ 11.0
ReSample	49.1 $\pm$ 0.8	16.3 $\pm$ 13.0
ReWeight	52.1 $\pm$ 4.7	10.0 $\pm$ 8.2
CBLoss	53.0 $\pm$ 3.2	13.3 $\pm$ 10.0
PDE	71.0 $\pm$ 12.6	8.3 $\pm$ 13.9
SCER	65.3 $\pm$ 1.0	<b>59.6 <math>\pm</math> 1.0</b>

In addition to the standard evaluation settings in Table 2, we examine a more challenging scenario in which a minority group is completely absent during training, creating a label color distribution of 50-0-10-40, as shown in Table 8. This extreme setting tests algorithms’ ability to generalize under harsh spurious correlations when facing complete group absence.

As shown in Table 3, SCER achieves 59.6% worst-group accuracy in this extreme setting, significantly outperforming all existing methods. This reveals limitations of existing approaches under extreme spurious correlations. In this extreme setting where an entire subpopulation is omitted from training, GroupDRO [Sagawa et al.] suffers from instability with extreme minority groups, poor extrapolation to unseen

subpopulations, and regularization-capacity trade-offs that limit its effectiveness. class imbalance methods [Japkowicz, 2000, Lin et al., 2017, Cui et al., 2019] and LISA [Yao et al., 2022] fail as they

rely on reweighting available samples or interpolating between seen domains, making them unable to handle completely missing groups. Similarly, PDE [Deng et al., 2023], despite initially learning from balanced data, cannot generalize to entirely unseen group combinations. These results demonstrate that under complete group absence, which induces extreme spurious correlations and corrupts the representation space, embedding-level interventions are essential. SCER’s superior performance is attributed to its direct regularization of the representation space, effectively mitigating spurious correlations and enabling robust generalization to entirely unseen subpopulations.

Table 4: Performance comparison without explicit bias labels on ColorMNIST.

ColorMNIST (Two train envs)	
Method	Avg Acc
IRM	54.8 $\pm$ 8.3
EIL (IRM)	58.5 $\pm$ 1.8
EIL + DRO	68.2 $\pm$ 7.0
EIL + SCER	<b>72.6 <math>\pm</math> 5.5</b>

**Integration with Environment Inference Methods.** A key advantage of SCER is its modular design, enabling seamless integration with existing frameworks without explicit bias labels. We integrate SCER with the Environment Inference for Invariant Learning (EIIL) framework [Creager et al., 2021], replacing EIIL’s second-stage IRM objective with SCER. Table 4 shows experimental results integrating EIIL with SCER where no environment information is provided, simulating realistic scenarios without environment labels. We adopt the data setup from [Creager et al., 2021] with two environments of different spurious correlation strengths, detailed in Table 8.

The environments inferred by EIIL achieve over 95% agreement with actual spurious groups in ColorMNIST, providing reliable pseudo-labels for SCER training. As shown in Table 4, SCER maintains its effectiveness even with inferred environments, achieving the highest test accuracy of 72.6%. Notably, while GroupDRO suffers significant performance degradation under environment misalignment, SCER remains robust due to its embedding-level regularization approach.

This demonstrates SCER’s practical applicability to real-world scenarios where explicit bias annotations are unavailable.

**Text Dataset** Table 5 presents SCER’s performance on text-based datasets. SCER consistently achieves the best results on both CivilComments for multi-domain evaluation and MultiNLI for multi-class evaluation. On CivilComments, SCER attains the highest worst-group accuracy of 74.0%, effectively mitigating minority subpopulation performance degradation. On MultiNLI, SCER achieves the highest worst-group accuracy of 76.8%, demonstrating balanced learning across different class distributions. These results confirm that SCER’s embedding regularization approach generalizes effectively beyond vision to text-based scenarios. SCER demonstrates robust performance across multi-domain and multi-class environments, highlighting its versatility in handling subpopulation shifts across modalities.

Table 5: Performance comparison on text datasets.  $\ddagger$  from Deng et al. [2023] for CivilComments.  $\dagger\dagger$  from Wen et al. [2025] for CivilComments. SCER achieves the best worst-group accuracy across multi-class and domain settings.

Algorithm	CivilComments		MultiNLI	
	Avg Acc	Worst Acc	Avg Acc	Worst Acc
ERM $^\dagger$	85.4 $\pm$ 0.2	63.7 $\pm$ 1.1	80.9 $\pm$ 0.1	66.8 $\pm$ 0.5
Mixup $^\dagger$	84.9 $\pm$ 0.3	66.1 $\pm$ 1.3	81.4 $\pm$ 0.3	68.5 $\pm$ 0.6
GroupDRO $^\dagger$	81.8 $\pm$ 0.6	70.6 $\pm$ 1.2	81.1 $\pm$ 0.3	76.0 $\pm$ 0.7
IRM $^\dagger$	85.5 $\pm$ 0.0	63.2 $\pm$ 0.8	77.8 $\pm$ 0.6	63.6 $\pm$ 1.3
CVaRDRO $^\dagger$	83.5 $\pm$ 0.3	68.7 $\pm$ 1.3	75.1 $\pm$ 0.1	63.0 $\pm$ 1.5
JTT $^\dagger$	83.3 $\pm$ 0.1	64.3 $\pm$ 1.5	80.9 $\pm$ 0.5	69.1 $\pm$ 0.1
LIF $^\dagger$	65.5 $\pm$ 5.6	51.0 $\pm$ 6.1	71.7 $\pm$ 1.1	63.6 $\pm$ 2.9
LISA $^\dagger$	82.7 $\pm$ 0.1	73.7 $\pm$ 0.3	80.3 $\pm$ 0.4	73.3 $\pm$ 1.0
MMD $^\dagger$	84.6 $\pm$ 0.2	54.5 $\pm$ 1.4	78.8 $\pm$ 0.1	69.1 $\pm$ 1.5
ReSample $^\dagger$	82.2 $\pm$ 0.0	73.3 $\pm$ 0.5	77.2 $\pm$ 0.2	72.3 $\pm$ 0.8
ReWeight $^\dagger$	82.5 $\pm$ 0.0	72.5 $\pm$ 0.0	81.0 $\pm$ 0.2	68.8 $\pm$ 0.4
SqrteReWeight $^\dagger$	83.3 $\pm$ 0.5	71.7 $\pm$ 0.4	80.7 $\pm$ 0.3	69.5 $\pm$ 0.7
CBLoss $^\dagger$	82.9 $\pm$ 0.1	73.3 $\pm$ 0.2	80.6 $\pm$ 0.1	72.2 $\pm$ 0.3
Focal $^\dagger$	85.5 $\pm$ 0.2	62.0 $\pm$ 1.0	80.7 $\pm$ 0.2	69.4 $\pm$ 0.7
LDAM $^\dagger$	81.9 $\pm$ 2.2	37.4 $\pm$ 8.1	80.7 $\pm$ 0.3	69.6 $\pm$ 1.6
BSoftmax $^\dagger$	83.8 $\pm$ 0.0	71.2 $\pm$ 0.4	80.9 $\pm$ 0.1	66.9 $\pm$ 0.4
DFR $^\dagger$	83.3 $\pm$ 0.0	69.6 $\pm$ 0.2	81.7 $\pm$ 0.0	68.5 $\pm$ 0.2
PDE $^\ddagger$	86.3 $\pm$ 1.7	71.5 $\pm$ 0.5	69.1 $\pm$ 0.3	65.8 $\pm$ 0.6
EIRRep $^{\dagger\dagger}$	79.0 $\pm$ 0.7	70.5 $\pm$ 0.5	69.0 $\pm$ 3.8	66.8 $\pm$ 5.2
SCER	81.7 $\pm$ 0.4	<b>74.0 <math>\pm</math> 1.0</b>	80.4 $\pm$ 0.1	<b>76.8 <math>\pm</math> 0.5</b>

## 5.2 Qualitative Analysis

**Embedding Regularization Analysis** We conduct sensitivity analysis on ColorMNIST with  $\rho = 95\%$  to evaluate our proposed loss components. As shown in Table 6, we systematically vary  $\lambda_{\text{core}}$  and  $\lambda_{\text{spur}}$  according to Equation 2. Results show each component independently improves worst-group accuracy, while their joint optimization achieves the highest robustness, confirming that  $\mathcal{L}_{\text{core}}$  and  $\mathcal{L}_{\text{spur}}$  produce complementary effects, validating our theoretical motivation. Additional analysis on CelebA is in Appendix C.

Table 6: Sensitivity analysis of embedding regularization on ColorMNIST. worst-group accuracy remains stable across settings, with the best results observed when both loss terms are combined.

ColorMNIST ( $\rho = 95\%$ )								
Setting	both $\lambda = 0$		$\lambda_{\text{core}}$ (fixed $\lambda_{\text{spur}}$ )			$\lambda_{\text{spur}}$ (fixed $\lambda_{\text{core}}$ )		
	Avg Acc	Worst Acc	$\lambda_{\text{core}}$	Avg Acc	Worst Acc	$\lambda_{\text{spur}}$	Avg Acc	Worst Acc
0	$72.3 \pm 0.1$	$70.7 \pm 0.2$	0.0	$72.8 \pm 0.4$	$71.6 \pm 0.6$	0.0	$72.8 \pm 0.3$	$71.6 \pm 0.4$
-	-	-	0.5	$73.0 \pm 0.2$	<b><math>72.2 \pm 0.4</math></b>	0.5	$72.3 \pm 0.4$	$71.6 \pm 0.3$
-	-	-	1.0	$73.3 \pm 0.2$	$72.0 \pm 0.2$	1.0	$73.5 \pm 0.3$	<b><math>72.8 \pm 0.3</math></b>

Table 7: Comparison between Euclidean norm and  $\Sigma$ -norm on ColorMNIST. Our proposed  $\Sigma$ -norm consistently achieves higher worst-group accuracy.

ColorMNIST ( $\rho = 95\%$ )		
Norm Type	Avg Acc	Worst Acc
Euclidean norm	$72.7 \pm 0.8$	$70.0 \pm 0.4$
$\Sigma$ -norm (Ours)	$73.5 \pm 0.3$	<b><math>72.8 \pm 0.3</math></b>

**Component Analysis** We investigate our proposed  $\Sigma$ -norm, also known as the Mahalanobis distance, by replacing the standard Euclidean norm in Equation 1. As shown in Table 7, the  $\Sigma$ -norm outperforms the Euclidean baseline. This improvement comes from the natural benefits of Mahalanobis distance, which captures the structure of covariance of the features and ensures the invariance of the scale in high-dimensional spaces [Ghorbani, 2019, Mahalanobis, 2018].

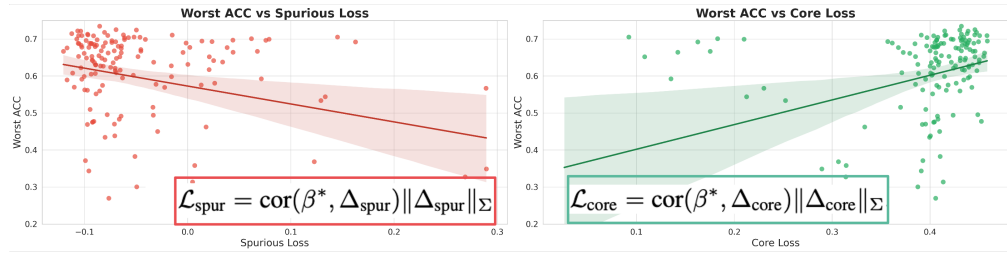


Figure 3: Scatter plots showing worst-group accuracy vs spurious and core metrics. Spurious Loss shows negative correlation, while Core Loss shows positive correlation.

#### Correlation Analysis between Objective Function Decomposition and worst-group accuracy

Figure 3 demonstrates the relationship between worst-group accuracy and spurious/core metrics, revealing insights into group-invariant learning. Spurious Loss exhibits negative correlations with Worst Acc, indicating that stronger classifier dependence on domain-specific characteristics degrades minority group performance, while Core Loss shows positive correlations, demonstrating that alignment with genuine label-discriminative features enhances cross-group generalization. Specifically, Weight-Spurious Alignment  $\text{cor}(\beta^*, \Delta_{\text{spur}})$  measures how much classifier weights align with intra-class domain variations, quantifying spurious feature dependence, while Weight-Core Alignment  $\text{cor}(\beta^*, \Delta_{\text{core}})$  captures how well the classifier aligns with domain-consistent discriminative directions. Spurious Magnitude  $\|\Delta_{\text{spur}}\|_{\Sigma}$  and Core Magnitude  $\|\Delta_{\text{core}}\|_{\Sigma}$  quantify inter-domain distributional differences and inter-label separability, respectively. These results establish that balancing core signal capture and spurious correlation suppression is fundamental to group invariance.

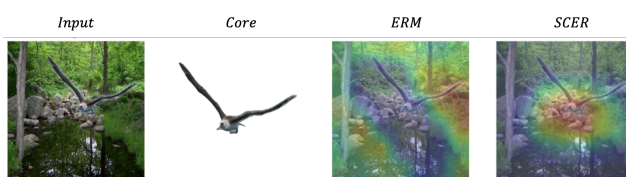


Figure 4: Comparison of Grad-CAM visualizations on the Waterbirds dataset. SCER directs attention to meaningful features, reducing focus on spurious regions.

**Grad-CAM** We compare ERM and SCER using Grad-CAM in Figure 4. ERM focuses on background regions, indicating spurious cue reliance. SCER consistently focuses on the bird itself, demonstrating that embedding regularization redirects attention to the true object and produces robust representations.

## 6 Conclusion

We propose Spurious Correlation-Aware Embedding Regularization (SCER), which addresses spurious correlations through embedding-level regularization that decomposes worst-group error into spurious and core components. SCER penalizes spurious feature alignment while promoting core feature consistency across domains, thereby mitigating spurious correlation overfitting. Experiments demonstrate superior worst-group accuracy, confirming SCER’s robust performance.

## References

Martin Arjovsky, Léon Bottou, Ishaan Gulrajani, and David Lopez-Paz. Invariant risk minimization. *arXiv preprint arXiv:1907.02893*, 2019.

Hyojin Bahng, Sanghyuk Chun, Sangdoo Yun, Jaegul Choo, and Seong Joon Oh. Learning de-biased representations with biased representations. In *International conference on machine learning*, pages 528–539. PMLR, 2020.

Daniel Borkan, Lucas Dixon, Jeffrey Sorensen, Nithum Thain, and Lucy Vasserman. Nuanced metrics for measuring unintended bias with real data for text classification. In *Companion proceedings of the 2019 world wide web conference*, pages 491–500, 2019.

Kaidi Cao, Colin Wei, Adrien Gaidon, Nikos Arechiga, and Tengyu Ma. Learning imbalanced datasets with label-distribution-aware margin loss. *Advances in neural information processing systems*, 32, 2019.

Elliot Creager, Jörn-Henrik Jacobsen, and Richard Zemel. Environment inference for invariant learning. In *International Conference on Machine Learning*, pages 2189–2200. PMLR, 2021.

Yin Cui, Menglin Jia, Tsung-Yi Lin, Yang Song, and Serge Belongie. Class-balanced loss based on effective number of samples. In *Proceedings of the IEEE/CVF conference on computer vision and pattern recognition*, pages 9268–9277, 2019.

Yihe Deng, Yu Yang, Baharan Mirzasoleiman, and Quanquan Gu. Robust learning with progressive data expansion against spurious correlation. *Advances in neural information processing systems*, 36:1390–1402, 2023.

John C Duchi and Hongseok Namkoong. Learning models with uniform performance via distributionally robust optimization. *The Annals of Statistics*, 49(3):1378–1406, 2021.

Hamid Ghorbani. Mahalanobis distance and its application for detecting multivariate outliers. *Facta Universitatis, Series: Mathematics and Informatics*, pages 583–595, 2019.

Ishaan Gulrajani and David Lopez-Paz. In search of lost domain generalization. *arXiv preprint arXiv:2007.01434*, 2020.

Yujin Han and Difan Zou. Improving group robustness on spurious correlation requires preciser group inference. In *International Conference on Machine Learning*, pages 17480–17504. PMLR, 2024.

Kaiming He, Xiangyu Zhang, Shaoqing Ren, and Jian Sun. Deep residual learning for image recognition. In *Proceedings of the IEEE conference on computer vision and pattern recognition*, pages 770–778, 2016.

Katherine Hermann and Andrew Lampinen. What shapes feature representations? exploring datasets, architectures, and training. *Advances in Neural Information Processing Systems*, 33:9995–10006, 2020.

Badr Youbi Idrissi, Martin Arjovsky, Mohammad Pezeshki, and David Lopez-Paz. Simple data balancing achieves competitive worst-group-accuracy. In *Conference on Causal Learning and Reasoning*, pages 336–351. PMLR, 2022.

Pavel Izmailov, Polina Kirichenko, Nate Gruver, and Andrew G Wilson. On feature learning in the presence of spurious correlations. *Advances in Neural Information Processing Systems*, 35:38516–38532, 2022.

Nathalie Japkowicz. The class imbalance problem: Significance and strategies. In *Proc. of the Int’l Conf. on artificial intelligence*, volume 56, pages 111–117, 2000.

Polina Kirichenko, Pavel Izmailov, and Andrew Gordon Wilson. Last layer re-training is sufficient for robustness to spurious correlations. In *ICML 2022: Workshop on Spurious Correlations, Invariance and Stability*.

Haoliang Li, Sinno Jialin Pan, Shiqi Wang, and Alex C Kot. Domain generalization with adversarial feature learning. In *Proceedings of the IEEE conference on computer vision and pattern recognition*, pages 5400–5409, 2018.

Weixin Liang and James Zou. Metashift: a dataset of datasets for evaluating contextual distribution shifts and training conflicts. In *International Conference on Learning Representations*, 2022.

Tsung-Yi Lin, Priya Goyal, Ross Girshick, Kaiming He, and Piotr Dollár. Focal loss for dense object detection. In *Proceedings of the IEEE international conference on computer vision*, pages 2980–2988, 2017.

Evan Z Liu, Behzad Haghighi, Annie S Chen, Aditi Raghunathan, Pang Wei Koh, Shiori Sagawa, Percy Liang, and Chelsea Finn. Just train twice: Improving group robustness without training group information. In Marina Meila and Tong Zhang, editors, *Proceedings of the 38th International Conference on Machine Learning*, volume 139 of *Proceedings of Machine Learning Research*, pages 6781–6792. PMLR, 18–24 Jul 2021. URL <https://proceedings.mlr.press/v139/liu21f.html>.

Ziwei Liu, Ping Luo, Xiaogang Wang, and Xiaoou Tang. Deep learning face attributes in the wild. In *Proceedings of International Conference on Computer Vision (ICCV)*, December 2015.

Ilya Loshchilov and Frank Hutter. Decoupled weight decay regularization. In *International Conference on Learning Representations (ICLR)*, 2019.

Prasanta Chandra Mahalanobis. On the generalized distance in statistics. *Sankhyā: The Indian Journal of Statistics, Series A* (2008-), 80:S1–S7, 2018.

Yifei Ming, Yiyou Sun, Ousmane Dia, and Yixuan Li. How to exploit hyperspherical embeddings for out-of-distribution detection? In *The Eleventh International Conference on Learning Representations*, 2023.

Junhyun Nam, Hyuntak Cha, Sungsoo Ahn, Jaeho Lee, and Jinwoo Shin. Learning from failure: De-biasing classifier from biased classifier. *Advances in Neural Information Processing Systems*, 33:20673–20684, 2020.

Rajvardhan Patil, Sorio Boit, Venkat Gudivada, and Jagadeesh Nandigam. A survey of text representation and embedding techniques in nlp. *IEEE Access*, 11:36120–36146, 2023.

Boris T Polyak. Some methods of speeding up the convergence of iteration methods. *USSR Computational Mathematics and Mathematical Physics*, 4(5):1–17, 1964.

Jiawei Ren, Cunjun Yu, Xiao Ma, Haiyu Zhao, Shuai Yi, et al. Balanced meta-softmax for long-tailed visual recognition. *Advances in neural information processing systems*, 33:4175–4186, 2020.

Shiori Sagawa, Pang Wei Koh, Tatsunori B Hashimoto, and Percy Liang. Distributionally robust neural networks. In *International Conference on Learning Representations*.

Shiori Sagawa, Aditi Raghunathan, Pang Wei Koh, and Percy Liang. An investigation of why overparameterization exacerbates spurious correlations. In *International Conference on Machine Learning*, pages 8346–8356. PMLR, 2020.

Baochen Sun and Kate Saenko. Deep coral: Correlation alignment for deep domain adaptation. In *Computer vision–ECCV 2016 workshops: Amsterdam, the Netherlands, October 8–10 and 15–16, 2016, proceedings, part III 14*, pages 443–450. Springer, 2016.

Vladimir Vapnik. *The nature of statistical learning theory*. Springer science & business media, 2013.

Catherine Wah, Steve Branson, Peter Welinder, Pietro Perona, and Serge Belongie. The caltech-ucsd birds-200-2011 dataset. 2011.

Tao Wen, Zihan Wang, Quan Zhang, and Qi Lei. Elastic representation: Mitigating spurious correlations for group robustness. In *International Conference on Artificial Intelligence and Statistics*, pages 541–549. PMLR, 2025.

Adina Williams, Nikita Nangia, and Samuel R Bowman. A broad-coverage challenge corpus for sentence understanding through inference. *arXiv preprint arXiv:1704.05426*, 2017.

Yu Yang, Besmira Nushi, Hamid Palangi, and Baharan Mirzasoleiman. Mitigating spurious correlations in multi-modal models during fine-tuning. In *International Conference on Machine Learning*, pages 39365–39379. PMLR, 2023a.

Yuzhe Yang, Haoran Zhang, Dina Katabi, and Marzyeh Ghassemi. Change is hard: a closer look at subpopulation shift. In *Proceedings of the 40th International Conference on Machine Learning*, pages 39584–39622, 2023b.

Huaxiu Yao, Yu Wang, Sai Li, Linjun Zhang, Weixin Liang, James Zou, and Chelsea Finn. Improving out-of-distribution robustness via selective augmentation. In *International Conference on Machine Learning*, pages 25407–25437. PMLR, 2022.

Wenqian Ye, Guangtao Zheng, Xu Cao, Yunsheng Ma, and Aidong Zhang. Spurious correlations in machine learning: A survey. *arXiv preprint arXiv:2402.12715*, 2024.

Hongyi Zhang, Moustapha Cisse, Yann N Dauphin, and David Lopez-Paz. mixup: Beyond empirical risk minimization. In *International Conference on Learning Representations*, 2018.

Bolei Zhou, Agata Lapedriza, Aditya Khosla, Aude Oliva, and Antonio Torralba. Places: A 10 million image database for scene recognition. *IEEE transactions on pattern analysis and machine intelligence*, 40(6):1452–1464, 2017.

## A Methodology

This section provides comprehensive algorithmic details and theoretical proofs for the SCER framework presented in the main paper. We first present detailed step-by-step procedures for the SCER implementation, including covariance computation, embedding regularization, and loss optimization that were summarized in the main text. Subsequently, we provide formal proofs for the theoretical foundations underlying our embedding regularization approach, including the decomposition of the embedding space into core and spurious components and the optimality conditions for robustness.

### A.1 Overall process of SCER

Recall from Section 3 that we define the Spurious and Core Loss as:

$$\mathcal{L}_{\text{spur}} = \text{cor}(\beta^*, \Delta_{\text{spur}}) \|\Delta_{\text{spur}}\|_{\Sigma}, \quad \mathcal{L}_{\text{core}} = \text{cor}(\beta^*, \Delta_{\text{core}}) \|\Delta_{\text{core}}\|_{\Sigma}.$$

The **Spurious Loss**  $\mathcal{L}_{\text{spur}}$  penalizes alignment with spurious directions, scaled by the magnitude of spurious variation in the data. The **Core Loss**  $\mathcal{L}_{\text{core}}$  encourages alignment with core directions, with the negative sign ensuring that stronger core alignment reduces the overall loss. Our loss formulation penalizes alignment with spurious directions and encourages alignment with core directions. By introducing control parameters  $\lambda_{\text{spur}}$  and  $\lambda_{\text{core}}$ , we derive our embedding loss function:

$$\mathcal{L}_{\text{embedding}} = \lambda_{\text{spur}} \mathcal{L}_{\text{spur}} - \lambda_{\text{core}} \mathcal{L}_{\text{core}}.$$

The final SCER objective combines embedding loss with worst-group classification loss  $\mathcal{L}_{\text{wge}}$ :

$$\mathcal{L}_{\text{total}} = \mathcal{L}_{\text{wge}} + \mathcal{L}_{\text{embedding}}.$$

This loss formulation mitigates overfitting to domain-specific biases by reducing intra-class variation across domains while preserving inter-class separability. SCER promotes robust decision boundaries, enabling strong worst-group performance under distribution shifts.

As shown in Equation 3, the total training loss combines two complementary components. The first term,  $\mathcal{L}_{\text{wge}}$ , is the worst-group classification loss derived from Group-DRO, which addresses subpopulation imbalances through robust optimization (**Worst-Group Error-based Classification**). The second term,  $\mathcal{L}_{\text{embedding}}$ , is an embedding-level regularization that explicitly controls the alignment between classifier weights and Spurious/Core Directions in the feature space (**Embedding-based Regularization**). This regularization penalizes the classifier’s reliance on domain-specific artifacts while encouraging alignment with label-consistent features. The two components work synergistically: the classification loss ensures robust performance across subpopulations, while the embedding regularization structures the representation space for better generalization. The combined objective is optimized via gradient-based methods (**Loss Optimization**). The details of each step are illustrated in Algorithm 1.

---

#### Algorithm 1 SCER Training Process

---

**Require:** Data  $(x, y)$ , parameters  $(w, \beta)$ , hyper-params  $(\eta, \lambda_{\text{spur}}, \lambda_{\text{core}})$   
**Initialize**  $q \leftarrow 1, \Sigma \leftarrow \mathbf{I}$   
**for** each step **do**  
 $x_{\text{emb}} \leftarrow f_w(x)$   
**(1) Worst-Group Error based Classification**  
 $\mathcal{L}(y, f_{\beta}(x_{\text{emb}})),$   
 $q_{(y,d)} \leftarrow q_{(y,d)} \exp(\eta \mathbb{E}[\mathcal{L}_{(y,d)}])$   
 $q \leftarrow q / \sum_{(y,d) \in \mathcal{Y} \times \mathcal{D}} q_{(y,d)}$   
 $\mathcal{L}_{\text{wge}} = \sum_{(y,d) \in \mathcal{Y} \times \mathcal{D}} q_{(y,d)} \mathbb{E}[\mathcal{L}_{(y,d)}]$   
**(2) Embedding-based Regularization**  
 $\Sigma = \frac{1}{N} \sum_i (x_{\text{emb},i} - \bar{x}_{\text{emb}})(x_{\text{emb},i} - \bar{x}_{\text{emb}})^T$   
 $\beta^* \leftarrow \text{current classifier weights}$   
 $\text{cor}(\beta^*, \Delta_{\text{spur}}) = \frac{1}{m} \sum_{j=1}^m \frac{\langle \beta_j^*, \Delta_{\text{spur}} \rangle}{\|\beta_j^*\|_{\Sigma} \|\Delta_{\text{spur}}\|_{\Sigma}}$   
 $\text{cor}(\beta^*, \Delta_{\text{core}}) = \frac{1}{m} \sum_{j=1}^m \frac{\langle \beta_j^*, \Delta_{\text{core}} \rangle}{\|\beta_j^*\|_{\Sigma} \|\Delta_{\text{core}}\|_{\Sigma}}$   
 $\mathcal{L}_{\text{spur}} = \text{cor}(\beta^*, \Delta_{\text{spur}}) \|\Delta_{\text{spur}}\|_{\Sigma}$   
 $\mathcal{L}_{\text{core}} = \text{cor}(\beta^*, \Delta_{\text{core}}) \|\Delta_{\text{core}}\|_{\Sigma}$   
 $\mathcal{L}_{\text{embedding}} = \lambda_{\text{spur}} \mathcal{L}_{\text{spur}} - \lambda_{\text{core}} \mathcal{L}_{\text{core}}$   
**(3) Optimize**  
 $\mathcal{L}_{\text{total}} = \mathcal{L}_{\text{wge}} + \mathcal{L}_{\text{embedding}}$   
Update  $(w, \beta)$  via gradient descent  
**end for**

---

**Worst-Group Error-based Classification.** The feature vector  $x_{\text{emb}} \in \mathbb{R}^p$ , where  $p$  is the embedding dimension, is used to compute classification losses for each group by comparing predictions with ground-truth labels. These group-wise losses are aggregated, and group-specific weights are updated using an exponentiated gradient scheme. This reweighting emphasizes underperforming groups, helping to correct distributional imbalances and enhancing robustness to worst-group errors.

**Embedding-based Regularization.** This step regularizes the learned representation by explicitly distinguishing spurious and core directions in the embedding space and aligning the decision boundary accordingly. To capture group-wise variability, a covariance matrix  $\Sigma \in \mathbb{R}^{p \times p}$  is computed from the feature embeddings  $x_{\text{emb}}$ . The core and spurious directions, denoted by  $\Delta_{\text{core}} \in \mathbb{R}^p$  and  $\Delta_{\text{spur}} \in \mathbb{R}^p$  respectively, are derived from the groupwise mean embeddings. To assess the classifier’s alignment with these directions, we use the current classifier weights  $\beta_j^* \in \mathbb{R}^p$  for each class  $j$ , which are dynamically updated during training via gradient descent. Using the weight matrix  $\beta^*$ , the spurious and core components— $\mathcal{L}_{\text{spur}}$  and  $\mathcal{L}_{\text{core}}$ —are computed, and their weighted combination forms the directional loss  $\mathcal{L}_{\text{embedding}}$ . Minimizing this objective reduces the classifier’s reliance on spurious directions while encouraging alignment with core directions, guiding the representation toward meaningful semantic structure. This regularization promotes intra-class alignment across domains and enhances inter-class separation, thereby mitigating spurious correlations in the embedding space and reducing worst-group error.

**Loss Optimization.** The total loss is computed by combining the worst-group-error loss  $\mathcal{L}_{\text{wge}}$  with the directional regularization loss  $\mathcal{L}_{\text{embedding}}$ . Minimizing this objective ensures that the classifier performs well across all groups while learning representations that are robust to spurious correlations. By aligning the embedding space with core directions and suppressing spurious ones, the method enhances robustness to worst-group errors under distribution shift.

## A.2 Theoretical Analysis of SCER

We now present a theoretical analysis that formally decomposes the worst-group error. Following prior work [Yao et al., 2022], we adopt a Gaussian mixture model to analyze how worst-group error arises from label-domain interactions.

### A.2.1 Binary Setting

Consider a classification problem where each data point  $x \in \mathcal{X}$  is associated with a label  $\mathcal{Y} = \{y_{-1}, y_{+1}\}$  and a domain  $\mathcal{D} = \{d_R, d_G\}$ . Each pair  $(y, d) \in \mathcal{Y} \times \mathcal{D}$  defines a *subpopulation*. We assume that the data follows a group-conditional Gaussian distribution  $x \mid (y, d) \sim \mathcal{N}(\mu^{(y, d)}, \Sigma)$  where  $\Sigma$  is positive definite. We further assume that  $\Delta_{\text{core}} = \mu^{(y_{+1}, d)} - \mu^{(y_{-1}, d)}$  is constant across  $d$ ,  $\Delta_{\text{spur}} = \mu^{(y, d_R)} - \mu^{(y, d_G)}$  is constant across  $y$ ,  $\Sigma^{(d_R)} = \Sigma^{(d_G)} = \Sigma$ ,  $\mathbb{P}(y = \pm 1) = \mathbb{P}(d \in \{d_R, d_G\}) = \frac{1}{2}$ , and  $\mathbb{P}_{y, d} \approx 0$  for some pairs  $(y, d)$  under extreme spurious correlations.

**Proposition 1** (ERM solution under Cross-Entropy Loss). *Under this assumption, the ERM solution with cross-entropy loss satisfies*

$$\beta^* \propto \Sigma^{-1} \tilde{\Delta}, \quad \tilde{\Delta} = \Delta_{\text{core}} + \Delta_{\text{spur}},$$

*Proof.* The ERM problem using cross-entropy loss as a logistic regression surrogate is

$$\min_{\beta, \beta_0} \mathbb{E}[\log(1 + \exp(-y(\beta^\top x + \beta_0)))].$$

The population minimizer  $\beta^*$  satisfies the score equation

$$\mathbb{E}[y x \sigma(-y(\beta^{*\top} x + \beta_0^*))] = 0, \quad \sigma(t) = \frac{1}{1+e^{-t}}.$$

Under the Gaussian assumption with shared covariance  $\Sigma$ , the Bayes classifier is derived from the log-likelihood ratio

$$\log \frac{p(x \mid y_{-1})}{p(x \mid y_{+1})} = (\mu^{(y_{-1})} - \mu^{(y_{+1})})^\top \Sigma^{-1} x - \frac{1}{2} (\mu^{(y_{-1})} + \mu^{(y_{+1})})^\top \Sigma^{-1} (\mu^{(y_{-1})} - \mu^{(y_{+1})}),$$

which is linear in  $x$  with a normal vector  $\Sigma^{-1}(\mu^{(y_{-1})} - \mu^{(y_{+1})})$ . Since logistic regression is Fisher-consistent under correct model specification, the cross-entropy minimizer  $\beta^*$  aligns with the Bayes direction:

$$\beta^* \propto \Sigma^{-1}(\mu^{(y_{-1})} - \mu^{(y_{+1})}).$$

In the extreme shift setting, the effective class means correspond to  $\mu^{(y_{-1}, d_R)}$  and  $\mu^{(y_{+1}, d_G)}$ . Thus

$$\beta^* \propto \Sigma^{-1}(\mu^{(y_{-1}, d_R)} - \mu^{(y_{+1}, d_G)}).$$

Decomposing the difference:

$$\mu^{(y_{-1}, d_R)} - \mu^{(y_{+1}, d_G)} = (\mu^{(y_{-1}, d_R)} - \mu^{(y_{+1}, d_R)}) + (\mu^{(y_{+1}, d_R)} - \mu^{(y_{+1}, d_G)}) = \Delta_{\text{core}} + \Delta_{\text{spur}} = \tilde{\Delta},$$

we conclude

$$\beta^* \propto \Sigma^{-1} \tilde{\Delta}.$$

□

**Theorem 1** (Worst-group error Decomposition). *Under this assumption, for classifier  $f_\beta = \text{sign}(\beta^{*\top} x)$  with  $\beta^* \in \mathbb{R}^p$ , the worst-group error can be decomposed as*

$$E_{\text{wge}} = \Phi\left(\pm \frac{1}{2} \text{cor}(\beta^*, \Delta_{\text{spur}}) \|\Delta_{\text{spur}}\|_\Sigma - \text{cor}(\beta^*, \Delta_{\text{core}}) \|\Delta_{\text{core}}\|_\Sigma\right),$$

*Proof.* Consider the linear classifier

$$f(x) = \text{sign}(\beta^\top x + \beta_0).$$

For subgroup  $(y, d)$ ,

$$\mathbb{P}(f(x) \neq y \mid (y, d)) = \Phi\left(-\frac{y(\beta^\top \mu^{(y, d)} + \beta_0)}{\|\beta\|_\Sigma}\right), \quad \|\beta\|_\Sigma = \sqrt{\beta^\top \Sigma \beta}.$$

Using  $\beta_0 = -\beta^\top \mathbb{E}[x]$  under extreme spurious correlations, we

$$\begin{aligned} E(y_{-1}, d_R) &= \Phi\left(-\frac{1}{2} \frac{\tilde{\Delta}^\top \beta}{\|\beta\|_\Sigma}\right), \\ E(y_{+1}, d_R) &= \Phi\left(\frac{-\Delta_{\text{core}}^\top \beta + \frac{1}{2} \tilde{\Delta}^\top \beta}{\|\beta\|_\Sigma}\right), \\ E(y_{-1}, d_G) &= \Phi\left(\frac{(\frac{1}{2} \tilde{\Delta} - \Delta_{\text{core}})^\top \beta}{\|\beta\|_\Sigma}\right), \\ E(y_{+1}, d_G) &= \Phi\left(\frac{\Delta_{\text{core}}^\top \beta - \frac{1}{2} \tilde{\Delta}^\top \beta}{\|\beta\|_\Sigma}\right). \end{aligned}$$

Let

$$z = \frac{1}{2} \frac{\tilde{\Delta}^\top \beta}{\|\beta\|_\Sigma}.$$

Then

$$E(y_{-1}, d_R) = \Phi(-z), \quad E(y_{+1}, d_G) = \Phi(z).$$

Since  $\Phi(-z) = 1 - \Phi(z)$ , one of these exceeds 0.5 while the other is below 0.5. The seen subgroups  $(y_{-1}, d_R), (y_{+1}, d_G)$  have arguments in  $[-z, z]$ , hence their errors lie in  $[\Phi(-z), \Phi(z)]$ .

$$E_{\text{wge}} = \max\{\Phi(-z), \Phi(z)\}.$$

Finally, writing  $\tilde{\Delta} = \Delta_{\text{spur}} + \Delta_{\text{core}}$  gives

$$E_{\text{wge}} = \Phi\left(\pm \frac{1}{2} \frac{\beta^\top \Delta_{\text{spur}}}{\|\beta\|_\Sigma} - \frac{\beta^\top \Delta_{\text{core}}}{\|\beta\|_\Sigma}\right).$$

With Proposition 1 and the identity

$$\frac{\beta^{*\top} v}{\|\beta^*\|_\Sigma} = \text{cor}(\beta^*, v) \|v\|_\Sigma,$$

The claimed expression follows. □

**Remark** The sign  $\pm$  appearing in Theorem 1 originates from the fact that the ERM solution Under cross-entropy loss is determined only up to an overall sign. That is, both  $\Sigma^{-1} \tilde{\Delta}$  and  $-\Sigma^{-1} \tilde{\Delta}$  define equivalent solutions, since the classifier depends only on the direction of  $\beta^*$ . Consequently, the  $\pm$  in the expression of the worst-group error does not alter the actual decision boundary or error behavior, but we retain it explicitly to make the sign ambiguity transparent.

## From Theoretical Analysis to Embedding Loss

From Theorem 1, the worst-group error under the Gaussian mixture model can be expressed as

$$E_{\text{wge}} = \Phi\left(\pm \frac{1}{2} \text{cor}(\beta^*, \Delta_{\text{spur}}) \|\Delta_{\text{spur}}\|_{\Sigma} - \text{cor}(\beta^*, \Delta_{\text{core}}) \|\Delta_{\text{core}}\|_{\Sigma}\right), \quad (4)$$

where  $\Phi(\cdot)$  is the standard Gaussian CDF.

Equation (4) shows that the worst-group error is governed by two competing components:

$$\underbrace{\text{cor}(\beta^*, \Delta_{\text{spur}}) \|\Delta_{\text{spur}}\|_{\Sigma}}_{\text{spurious term}} \quad \text{and} \quad \underbrace{\text{cor}(\beta^*, \Delta_{\text{core}}) \|\Delta_{\text{core}}\|_{\Sigma}}_{\text{core term}}.$$

The first term increases the error through alignment with spurious directions, while the second decreases the error through alignment with core directions. Thus, minimizing  $E_{\text{wge}}$  requires simultaneously suppressing the spurious term and enhancing the core term.

Motivated by this decomposition, we define the following surrogate regularizers:

$$\begin{aligned} \mathcal{L}_{\text{spur}} &= \text{cor}(\beta, \Delta_{\text{spur}}) \|\Delta_{\text{spur}}\|_{\Sigma}, \\ \mathcal{L}_{\text{core}} &= \text{cor}(\beta, \Delta_{\text{core}}) \|\Delta_{\text{core}}\|_{\Sigma}, \end{aligned}$$

where  $\beta$  denotes the classifier weights. The embedding-level regularization is then given by

$$\mathcal{L}_{\text{embedding}} = \lambda_{\text{spur}} \mathcal{L}_{\text{spur}} - \lambda_{\text{core}} \mathcal{L}_{\text{core}}. \quad (5)$$

**Remark.** In Appendix 1, we derived Eq. (4) under the strict ERM setting with Gaussian assumptions, where the optimal  $\beta^*$  has the closed form  $\beta^* \propto \Sigma^{-1} \tilde{\Delta}$ . In practice, however,  $\beta$  corresponds to the weight parameters of a deep neural classifier trained via stochastic optimization. While  $\beta$  may not coincide with the ERM minimizer, the decomposition in Eq. (4) remains structurally valid: worst-group error is still determined by the trade-off between spurious and core alignment. This observation justifies applying the embedding regularization loss in Eq. (5) to deep models.

### A.2.2 Multiclass/Multidomain Setting

We now generalize this assumption to multiclass, multidomain settings to investigate whether analogous results are preserved.

Consider a classification problem where each data point  $x \in \mathcal{X}$  is associated with a label  $\mathcal{Y} = \{y_1, \dots, y_m\}$  and a domain  $\mathcal{D} = \{d_1, \dots, d_k\}$ . Each pair  $(y, d) \in \mathcal{Y} \times \mathcal{D}$  defines a *subpopulation*. We assume that the data follows a group-conditional Gaussian distribution  $x \mid (y, d) \sim \mathcal{N}(\mu^{(y, d)}, \Sigma)$  where  $\Sigma$  is positive definite. We further assume that  $\Delta_{\text{core}}^{(i, j)} = \mu^{(y_i, d)} - \mu^{(y_j, d)}$  is constant across  $d$ ,  $\Delta_{\text{spur}}^{(i, j)} = \mu^{(y, d_i)} - \mu^{(y, d_j)}$  is constant across  $y$ ,  $\Sigma^{(d_1)} = \Sigma^{(d_2)} = \dots = \Sigma^{(d_k)} = \Sigma$ ,  $\mathbb{P}(y = y_i) = \frac{1}{m}$ ,  $\mathbb{P}(d = d_j) = \frac{1}{k}$ , and  $\mathbb{P}_{y, d} \approx 0$  for some pairs  $(y, d)$  under extreme spurious correlations, meaning that most samples from a given label class come from a specific domain.

**Proposition 2** (Multiclass/Multidomain ERM under Cross-Entropy Loss). *Under the assumptions, the ERM solution with multinomial logistic regression satisfies, for all  $i \neq j$ ,*

$$\beta_i^* - \beta_j^* \propto \Sigma^{-1} \tilde{\Delta}^{(i, j)}, \quad \tilde{\Delta}^{(i, j)} = \Delta_{\text{core}}^{(i, j)} + \Delta_{\text{spur}}^{(i, j)},$$

where  $d_p$  and  $d_q$  denote the predominant domains for classes  $y_i$  and  $y_j$ , respectively, under the extreme spurious-correlation assumption.

*Proof.* The ERM problem using cross-entropy loss for multinomial logistic regression is

$$\min_{\{(\beta_i, \beta_{0i})\}_{i=1}^m} \mathbb{E} \left[ - \sum_{i=1}^m \mathbf{1}\{y = i\} \log \frac{\exp(\beta_i^\top x + \beta_{0i})}{\sum_{r=1}^m \exp(\beta_r^\top x + \beta_{0r})} \right].$$

Assume the group-conditional Gaussian model with shared covariance,

$$x_{\text{emb}} \mid (y = i, d = j) \sim \mathcal{N}(\mu^{(y_i, d_j)}, \Sigma),$$

where  $\mu^{(y_i, d_j)} = \mathbb{E}_{x \sim \mathbb{P}_{y_i, d_j}} [f_w(x)]$  denotes the mean embedding of subpopulation  $(y_i, d_j)$ . Let  $\pi_i = \mathbb{P}(y = i)$  denote the class prior. The Bayes discriminant for class  $i$  is

$$\delta_i(x_{\text{emb}}) = x_{\text{emb}}^\top \Sigma^{-1} \bar{\mu}_i - \frac{1}{2} \bar{\mu}_i^\top \Sigma^{-1} \bar{\mu}_i + \log \pi_i,$$

where  $\delta_i(\cdot)$  denotes the LDA-type discriminant and  $\bar{\mu}_i$  the effective class mean. Then, for any  $i \neq j$ ,

$$\log \frac{p(y = i \mid x_{\text{emb}})}{p(y = j \mid x_{\text{emb}})} = (\bar{\mu}_i - \bar{\mu}_j)^\top \Sigma^{-1} x_{\text{emb}} - \frac{1}{2} (\bar{\mu}_i^\top \Sigma^{-1} \bar{\mu}_i - \bar{\mu}_j^\top \Sigma^{-1} \bar{\mu}_j) + \log \pi_i - \log \pi_j,$$

which is linear in  $x_{\text{emb}}$  with normal vector  $\Sigma^{-1}(\bar{\mu}_i - \bar{\mu}_j)$ . By Fisher consistency of multinomial logistic regression under the correctly specified linear logit model,

$$\beta_i^* - \beta_j^* \propto \Sigma^{-1}(\bar{\mu}_i - \bar{\mu}_j).$$

Under the extreme spurious-correlation assumption, each class  $y_i$  predominantly appears in a single domain  $d_p$ , hence

$$\bar{\mu}_i \approx \mu^{(y_i, d_p)}.$$

Based on this, we decompose

$$\bar{\mu}_i - \bar{\mu}_j \approx (\mu^{(y_i, d_p)} - \mu^{(y_j, d_p)}) + (\mu^{(y_j, d_p)} - \mu^{(y_j, d_q)}) = \Delta_{\text{core}}^{(i,j)} + \Delta_{\text{spur}}^{(p,q)}.$$

Substituting into the previous relation gives

$$\beta_i^* - \beta_j^* \propto \Sigma^{-1} \left( \Delta_{\text{core}}^{(i,j)} + \Delta_{\text{spur}}^{(p,q)} \right).$$

□

**Theorem 2** (Multiclass/Multidomain Worst-Group error). *Under these assumptions, for the softmax classifier be parameterized by  $\{(\beta_i, \beta_{0i})\}_{i=1}^m$  and define the pairwise standardized margin on subgroup  $(y_i, d_p)$  against class  $i \neq j$  as*

$$m_{i \rightarrow j}(\beta) := \frac{(\beta_i - \beta_j)^\top \mu^{(y_i, d_p)} + (\beta_{0i} - \beta_{0j})}{\|\beta_i - \beta_j\|_\Sigma}.$$

Then the subgroup error is bounded as

$$\max_{i \neq j} \Phi(-m_{i \rightarrow j}(\beta)) \leq \mathbb{P}(f(x_{\text{emb}}) \neq i \mid y = y_i, d = d_p) \leq \sum_{i \neq j} \Phi(-m_{i \rightarrow j}(\beta)),$$

and the worst-group error over observed subgroups satisfies

$$\max_i \max_{i \neq j} \Phi(-m_{i \rightarrow j}(\beta)) \leq E_{\text{wge}}(\beta) \leq \max_i \sum_{i \neq j} \Phi(-m_{i \rightarrow j}(\beta)).$$

*Proof.* Fix  $(y = y_i, d = d_p)$ . Since  $x_{\text{emb}} \sim \mathcal{N}(\mu^{(y_i, d_p)}, \Sigma)$ , the pairwise score difference

$$T_{i \rightarrow j}(x_{\text{emb}}) := (\beta_i - \beta_j)^\top x_{\text{emb}} + (\beta_{0i} - \beta_{0j})$$

is Gaussian with mean  $(\beta_i - \beta_j)^\top \mu^{(y_i, d_p)} + (\beta_{0i} - \beta_{0j})$  and variance  $\|\beta_i - \beta_j\|_\Sigma^2$ . Hence

$$\mathbb{P}(\text{misclassify } i \text{ as } j \mid y = y_i, d = d_p) = \Phi(-m_{i \rightarrow j}(\beta)).$$

The lower bound follows from  $\mathbb{P}(\cup_{i \neq j} A_j) \geq \max_j \mathbb{P}(A_j)$  and the upper bound from the union bound  $\mathbb{P}(\cup_{i \neq j} A_j) \leq \sum_j \mathbb{P}(A_j)$ . □

### From Theoretical Analysis to Embedding Loss (Multiclass/Multidomain)

Under Proposition 2, the population ERM solution satisfies  $\beta_i^* - \beta_j^* \propto \Sigma^{-1} \tilde{\Delta}_{i,j}$  with  $\tilde{\Delta}_{i,j} := \Delta_{\text{core}}^{(i,j)} + \Delta_{\text{spur}}^{(p,q)}$ . With balanced class priors, the corresponding biases yield  $m_{i \rightarrow j}(\beta^*) = \frac{1}{2} \|\tilde{\Delta}_{i,j}\|_\Sigma$ , so that

$$\max_i \max_{i \neq j} \Phi\left(-\frac{1}{2} \|\tilde{\Delta}_{i,j}\|_\Sigma\right) \leq E_{\text{wge}}(\beta^*) \leq \max_i \sum_{i \neq j} \Phi\left(-\frac{1}{2} \|\tilde{\Delta}_{i,j}\|_\Sigma\right).$$

Equivalently, in directional form,

$$\|\tilde{\Delta}_{i,j}\|_{\Sigma} = \left\| \Delta_{\text{core}}^{(i,j)} + \Delta_{\text{spur}}^{(p,q)} \right\|_{\Sigma} = \left\| \text{cor}(\cdot, \Delta_{\text{core}}^{(i,j)}) \|\Delta_{\text{core}}^{(i,j)}\|_{\Sigma} + \text{cor}(\cdot, \Delta_{\text{spur}}^{(p,q)}) \|\Delta_{\text{spur}}^{(p,q)}\|_{\Sigma} \right\|,$$

where “.” denotes  $\beta_i^* - \beta_j^*$  normalized in the  $\Sigma$ -inner product.

We observe that the sign of the spurious term can vary across domain pairs  $(p, q)$ . A worst-case treatment therefore selects the least favorable sign, yielding

$$\min_{(p,q)} \text{cor}(\cdot, \Delta_{\text{spur}}^{(p,q)}) \|\Delta_{\text{spur}}^{(p,q)}\|_{\Sigma} = - \max_{(p,q)} |\text{cor}(\cdot, \Delta_{\text{spur}}^{(p,q)})| \|\Delta_{\text{spur}}^{(p,q)}\|_{\Sigma}.$$

Consequently, a conservative lower bound on the pairwise margin is given by

$$\underbrace{\text{cor}(\cdot, \Delta_{\text{core}}^{(i,j)}) \|\Delta_{\text{core}}^{(i,j)}\|_{\Sigma}}_{\text{beneficial to increase}} - \underbrace{\max_{(p,q)} |\text{cor}(\cdot, \Delta_{\text{spur}}^{(p,q)})| \|\Delta_{\text{spur}}^{(p,q)}\|_{\Sigma}}_{\text{beneficial to decrease}}.$$

This decomposition shows that worst-case group-wise margin can be improved by increasing alignment with the core direction while reducing absolute alignment with spurious directions. When combined with the pairwise margin bounds from Theorem 2, this leads to a tighter worst-group error bound by simultaneously raising the lower bound and lowering the upper bound.

Based on this analysis, the SCER framework integrates three key components: (1) Worst-Group Error-based Classification using group-dependent loss weighting, (2) Embedding-based Regularization that identifies and scales core and spurious components through covariance analysis, and (3) Loss Optimization with embedding regularization. This approach effectively mitigates spurious correlations while enhancing class separation, improving robustness under distribution shifts without compromising performance. SCER implements this through regularization terms that control directional correlations, providing a principled approach to robust classification. In conclusion, SCER mitigates spurious correlations by regularizing embedding directions to reduce reliance on spurious features while strengthening core predictive signals. This approach effectively improves worst-group accuracy and enhances robustness under distribution shifts across diverse datasets and modalities.

## B Experimental Setup

### B.1 Experimental Setting

This section provides comprehensive details of our experimental configuration for evaluating the SCER framework. We describe the datasets used for evaluation, model architectures employed across different domains, baseline methods for comparison, hyperparameter settings, and evaluation metrics. These detailed specifications ensure reproducibility and provide a complete context for the results presented in the main paper.

#### B.1.1 Datasets

We conduct experiments on six benchmark datasets: four image datasets (Waterbirds, CelebA, MetaShift, ColorMNIST) and two text datasets (CivilComments, MultiNLI). These datasets are established benchmarks for evaluating model robustness against spurious correlations. Dataset characteristics and statistics are summarized in Table 8.

**Waterbirds** Waterbirds [Sagawa et al.] is a binary classification dataset constructed by superimposing bird images from the CUB dataset [Wah et al., 2011] onto backgrounds from the Places dataset [Zhou et al., 2017]. The task involves classifying images as landbirds or waterbirds, where background type creates spurious correlations between land backgrounds and landbirds, and water backgrounds and waterbirds. We use the standard data splits from Idrissi et al. [2022].

**CelebA** CelebA [Liu et al., 2015] contains approximately 200,000 celebrity images. We formulate the problem as a binary classification, classifying hair as either blond or not blond, with gender serving as the spurious attribute. We follow the standard splits from Idrissi et al. [2022].

Table 8: Statistics of datasets. For ColorMNIST,  $\rho$  denotes the spurious correlation level between label  $y$  and domain attribute (color) in the training set. A higher  $\rho$  indicates stronger spurious correlation, making color a more predictive but misleading cue for classification. "One Subpopulation Omitted" represents an extreme case where one group combination is completely absent from training data. Groups are defined as combinations of class labels and attribute values, and Max/Min group columns show the sample sizes of the largest and smallest groups, respectively. The disparity between these values indicates the degree of group imbalance, which tests model robustness under uneven data distribution.

Dataset	Data type	# Attr.	# Classes	# Train	# Val.	# Test	Max group	Min group
Waterbirds	Image	2	2	4,795	1,199	5,794	3,498	56
CelebA	Image	2	2	162,770	19,867	19,962	71,629	1,387
MetaShift	Image	2	2	2,276	349	874	789	196
<b>ColorMNIST</b>								
$\rho = 80\%$	Image	2	2	30,000	10,000	20,000	12,228	3,002
$\rho = 90\%$	Image	2	2	30,000	10,000	20,000	13,756	1,469
$\rho = 95\%$	Image	2	2	30,000	10,000	20,000	14,518	731
One Subpopulation Omitted	Image	2	2	30,000	10,000	20,000	15,249	0
Two train envs	Image	2	2	50,000	0	10,000	21,529	3,644
- env1 ( $\rho = 80\%$ )	Image	2	2	25,000	0	0	10,117	2,415
- env2 ( $\rho = 90\%$ )	Image	2	2	25,000	0	0	11,412	1,229
CivilComments	Text	8	2	148,304	24,278	71,854	31,282	1,003
MultiNLI	Text	2	3	206,175	82,462	123,712	67,376	1,521

**MetaShift** From the MetaShift benchmark [Liang and Zou, 2022], we use the Cats vs. Dogs binary classification task, where background type serves as the spurious attribute through correlations between indoor backgrounds with cats and outdoor backgrounds with dogs. We adopt the unmixed version provided by the dataset authors.

**ColorMNIST** ColorMNIST [Arjovsky et al., 2019] is a synthetic variant of MNIST where each digit is assigned a color. The classification task groups digits into two categories: zero and four versus five and nine, with color serving as the spurious attribute through red and green assignments. Training data exhibits strong color-class correlations, validation data is balanced at 50:50, and test data reverses the correlation pattern to 10:90. Following Arjovsky et al. [2019], we inject 25% label noise and evaluate under varying spurious correlation strengths of 80:20, 90:10, and 95:5 ratios to assess robustness.

To test the limits of group imbalance, we conducted additional experiments on ColorMNIST with severe distributional skew where one subpopulation is completely omitted from training. Specifically, we use 15,249 samples for Label 0 with Color 0, 3,000 samples for Label 1 with Color 0, and 11,751 samples for Label 1 with Color 1, while Label 0 with Color 1 contains 0 samples. This extreme setting evaluates model performance when certain subpopulations are entirely missing during training, representing a challenging scenario for robust classification methods.

To test the generalizability of SCER, we conducted additional experiments on ColorMNIST using the environment inference methodology from Creager et al. [2021]. Following the prior protocol with two environments in train, we partition the dataset into 50,000 training samples and 10,000 test samples. The training set is further divided into two environments, each containing 25,000 samples, representing different spurious correlation patterns. We maintain consistency with our primary experimental setup by using identical model architectures, training procedures, and evaluation metrics across all experiments.

**CivilComments** CivilComments [Borkan et al., 2019] provides a binary text classification benchmark designed to identify toxic language in online comments. Mentions of demographic groups serve as spurious attributes. We use the standard WILDS splits.

**MultiNLI** The MultiNLI dataset [Williams et al., 2017] addresses natural language inference by requiring models to classify the relationship between a premise and a hypothesis as entailment, contradiction, or neutrality. The presence of negation words serves as a confounding factor because

Table 9: Hyperparameters and search spaces.

Model / Method	Hyperparameter	Default, Search Space
<b>Base Models</b>		
ResNet	Learning rate	0.001, $10^{\text{Uniform}(-4, -2)}$
	Batch size	108, $2^{\text{Uniform}(6, 7)}$
BERT	Learning rate	$10^{-5}$ , $10^{\text{Uniform}(-5.5, -4)}$
	Batch size	32, $2^{\text{Uniform}(3, 5.5)}$
	Dropout	0.5, <code>RandomChoice([0, 0.1, 0.5])</code>
<b>Subpopulation Robustness Methods</b>		
GroupDRO	$\eta$	0.01, $10^{\text{Uniform}(-3, -1)}$
CVaRDRO	$\alpha$	0.1, $10^{\text{Uniform}(-2, 0)}$
LfF	$q$	0.7, $\text{Uniform}(0.05, 0.95)$
JTT	First-stage step fraction	0.5, $\text{Uniform}(0.2, 0.8)$
	$\lambda$	10, $10^{\text{Uniform}(0, 2.5)}$
LISA	$\alpha$	2, $10^{\text{Uniform}(-1, 1)}$
	$p_{\text{select}}$	0.5, $\text{Uniform}(0, 1)$
DFR	Regularization	0.1, $10^{\text{Uniform}(-2, 0.5)}$
ElRep	$\theta_1, \theta_2$	0.1, $\text{Uniform}(0, 1)$
<b>Domain-Invariant Methods</b>		
IRM	$\lambda$	100, $10^{\text{Uniform}(-1, 5)}$
	Iterations of penalty annealing	500, $10^{\text{Uniform}(0, 4)}$
MMD	$\gamma$	1, $10^{\text{Uniform}(-1, 1)}$
<b>Data Augmentation</b>		
Mixup	$\alpha$	0.2, $10^{\text{Uniform}(0, 4)}$
<b>Class Imbalance Methods</b>		
ReSample	–	Follow default implementation
ReWeight	–	Follow default implementation
SqrtWeight	–	Follow default implementation
Focal Loss	$\gamma$	$1, 0.5 \times 10^{\text{Uniform}(0, 1)}$
CBLoss	$\beta$	0.9999, $1 - 10^{\text{Uniform}(-5, -2)}$
LDAM	max_m	0.5, $10^{\text{Uniform}(-1, -0.1)}$
	scale	30, <code>RandomChoice([10, 30])</code>
<b>Proposed Method (SCER)</b>		
SCER	$\eta$	0.01, $10^{\text{Uniform}(-3, -1)}$
	$\lambda_{\text{core}}$	1, $\text{Uniform}(0, 1)$
	$\lambda_{\text{spur}}$	1, $\text{Uniform}(0, 1)$

they exhibit a strong correlation with contradiction labels. We adopt the data splits established in Idrissi et al. [2022].

### B.1.2 Baselines

For fair comparison, we followed the training protocol of Gulrajani and Lopez-Paz [2020], performing random search over each method’s joint hyperparameter space. Hyperparameter configurations follow prior work [Yang et al., 2023b] for all baseline methods. We selected the hyperparameters that achieved the highest Worst Accuracy for each algorithm, then conducted three independent runs with different random seeds (0, 1, 2) to account for variance and ensure robustness of reported results. Final average performance and standard deviation are reported across these runs. Complete hyperparameter details are provided in Table 9 summarizes the hyperparameters used for each baseline. In addition to standard optimization parameters such as batch size, learning rate, and dropout, we include key weighting parameters  $\eta$ ,  $\lambda_{\text{spur}}$ , and  $\lambda_{\text{core}}$ , which are used to suppress spurious features and enhance core features. These values are chosen to encourage the model to learn generalizable representations under distribution shifts. To comprehensively evaluate the robustness of our method, we compare its performance against a wide range of baselines, including standard ERM, subpopulation robustness methods, domain-invariant approaches, data augmentation techniques, and class imbalance methods.

**Empirical Risk Minimization** ERM minimizes the average loss over all training samples without explicitly addressing group-specific performance disparities.

**subpopulation Robustness Methods** GroupDRO [Sagawa et al.] is a representative approach to distributional robustness that improves worst-group performance by assigning greater importance to groups with higher losses. CVaRDRO [Duchi and Namkoong, 2021] extends this approach to the individual sample level, enabling more fine-grained adjustment by assigning importance weights to individual samples. Lff [Nam et al., 2020] employs a co-training approach that simultaneously trains a biased model and a debiased model, guiding the model to learn by distinguishing between biased and unbiased features. JTT [Liu et al., 2021] is a two-stage strategy that identifies hard samples using information obtained from initial standard empirical risk minimization (ERM) training, then improves model robustness by increasing the weights of these samples in the second training stage. LISA [Yao et al., 2022] utilizes data augmentation techniques that mix data within and across attributes, encouraging the model to learn invariant features of attributes. DFR [Kirichenko et al.] is an efficient method that improves robustness by retraining only the last layer using a balanced validation set, rather than the entire model. PDE [Deng et al., 2023] employs a strategy of progressively expanding training data, guiding the model to first focus on core features and subsequently learn spurious features. Finally, ERep [Wen et al., 2025] introduces both Nuclear-norm and Frobenius-norm regularization to representation vectors, enabling robust group generalization representation learning against spurious correlations by simultaneously emphasizing important features and maintaining diversity.

**Domain-Invariant Methods** IRM [Arjovsky et al., 2019] is a method for finding invariant predictors that work commonly across multiple domains. Specifically, it trains feature extractors such that a fixed predictor becomes optimal in each domain, enabling the model to effectively capture important characteristics regardless of domain changes. This approach ensures robust performance even when domains change. MMD [Li et al., 2018] is a method that numerically measures the difference in feature distributions between different domains, training to reduce this difference to mitigate distribution mismatches across domains. In other words, it is an approach that aims to improve generalization performance by making feature representations across domains as similar as possible.

**Data Augmentation** Mixup [Zhang et al., 2018] is a technique that creates new synthetic training data by linearly interpolating two random samples and their labels. This smooths decision boundaries and serves as regularization to improve generalization performance and prevent overfitting. It is a simple yet effective data augmentation method that artificially expands training data diversity by learning intermediate points between samples in the data space.

**Class Imbalance Methods** ReSample [Japkowicz, 2000] mitigates class imbalance in training data through resampling techniques. ReWeight [Japkowicz, 2000] assigns weights to the loss function proportional to class frequency. SQRTWeight is another loss adjustment method that modifies loss weights using the inverse square root of class frequency, appropriately increasing the influence of minority classes in imbalanced data. Focal Loss [Lin et al., 2017] focuses on difficult samples by reducing the contribution of easy-to-learn samples. CB Loss [Cui et al., 2019] calculates sample weights based on effective class size. LDAM [Cao et al., 2019] assigns different margins for each class to balance decision boundaries. Balanced Softmax [Ren et al., 2020] modifies the softmax function itself to accommodate class imbalance.

We compared our model against these numerous baselines and demonstrated the superiority of our approach, confirming the necessity of embedding regularization.

## C Additional experiment

This section presents supplementary experimental results that further validate the effectiveness and robustness of the SCER framework.

### C.1 Quantitative Analysis

We conduct a comprehensive quantitative analysis to evaluate the computational complexity and scalability of the SCER framework. These experiments provide detailed insights into SCER’s adaptation mechanisms across various scenarios and assess its practical feasibility for real-world deployment.

Table 10: Average per-iteration training time (seconds).

Method	Avg One Iteration (s)
ERM	0.0654
GroupDRO	0.0915
DFR	0.1025
SCER	0.0988

**Complexity analysis** While our method requires computational investment for correlation metric and mean embedding computations, it maintains computational costs comparable to established robust training methods. As shown in Table 10, our approach requires 0.0988 seconds per iteration, which is marginally higher than GroupDRO at 0.0915 seconds but significantly faster than the two-stage DFR method at 0.1025 seconds.

Importantly, DFR’s computational overhead stems from its inherent two-stage paradigm [Kirichenko et al.]: first training with ERM to learn representations, then retraining only the final layer with group-balanced data. This approach suffers from critical limitations, including the requirement for high-quality, balanced validation data and complete failure when ERM cannot capture core features, such as when minority groups are entirely absent from training data. In contrast, our single-stage approach achieves substantially better worst-group accuracy than these alternatives while avoiding DFR’s structural constraints. Most importantly, our method requires no balanced validation data or multistage training, delivering superior robustness with greater practical simplicity.

Table 11: Sensitivity analysis of embedding regularization on CelebA. Worst-group accuracy remains relatively stable across settings, with the best results observed when moderate  $\lambda_{\text{core}}$  is applied.

CelebA									
both $\lambda = 0$			$\lambda_{\text{core}}$ (fixed $\lambda_{\text{spur}}$ )			$\lambda_{\text{spur}}$ (fixed $\lambda_{\text{core}}$ )			
Setting	Avg Acc	Worst Acc	$\lambda_{\text{core}}$	Avg Acc	Worst Acc	$\lambda_{\text{spur}}$	Avg Acc	Worst Acc	
0	$91.4 \pm 0.6$	$89.0 \pm 0.7$	0.0	$92.5 \pm 0.1$	$91.1 \pm 0.2$	0.0	$92.0 \pm 0.3$	<b><math>91.0 \pm 0.2</math></b>	
–	–	–	0.5	$92.7 \pm 0.2$	<b><math>91.4 \pm 0.1</math></b>	0.5	$91.7 \pm 0.6$	$90.9 \pm 0.7$	
–	–	–	1.0	$92.7 \pm 0.2$	$90.9 \pm 0.5$	1.0	$92.0 \pm 0.1$	$90.7 \pm 0.1$	

### C.2 Qualitative Analysis

We provide comprehensive quantitative evaluations including additional sensitivity analysis across hyperparameters.

**Embedding Regularization Analysis** In addition to the results in Table 6, we conduct sensitivity analysis for  $\lambda_{\text{core}}$  and  $\lambda_{\text{spur}}$  on the large-scale real-world dataset CelebA. The results confirm the generalizability of our ColorMNIST findings beyond synthetic settings. CelebA exhibits even more pronounced performance improvements with appropriate hyperparameter values, highlighting the effectiveness of embedding regularization in mitigating spurious correlations in realistic scenarios, as shown in Table 11

## D Statement on the Use of Large Language Models

Large Language Models (LLMs) were used in limited capacity during the preparation of this research. Specifically, LLMs were used to check grammar and refine sentence structure after the initial draft was completed, primarily to correct awkward expressions and maintain consistency in writing style. However, all core research ideas, analytical methodologies, interpretations of the results, and conclusions were developed entirely by the authors. The LLM did not contribute to any creative content or academic judgments. This use of LLMs was conducted within limits that do not compromise the originality or academic integrity of the research.